University of Crete
School of Sciences and Engineering
Department of Mathematics and Applied Mathematics

Structure of Magnetic Materials with Monte Carlo Methods

Author:
Michaela-Areti Zervou

Supervisors:
Euangelos Harmandaris
Stavros Komineas

A thesis submitted in fulfillment of the requirements for the degree of Master of Science

July 2016

Abstract

Recent observations of chiral structures in magnetic thin films have raised a great interest for the Dzyaloshinskii-Moriya interaction (DMI), as it favors magnetization rotations with a fixed chirality. This coupling originates from the combination of low structural symmetry and large spin-orbit coupling. It has been first proposed in bulk materials lacking space inversion symmetry but it also exists at the interface between a magnetic film and a high spin-orbit coupling adjacent layer.

The aim of this thesis concerns the theoretical and computational study of the modification of micromagnetic configurations in magnetic materials, due to the presence of Dzyaloshinskii-Moriya interaction (DMI)and the easy-axis anisotropy that appears at the interface of an ultrathin film. We explore several cases of ultrathin film structures that allow analytical calculations (1D systems,domain walls and spirals), compared with numerical calculations. For the numerical calculations we analyzed a discretized version of a widely used continuum model that describes a magnet Dzyaloshinskii-Moriya interaction (DMI)and the easy-axis anisotropy. Single-flip Metropolis Monte Carlo methods are applied to describe those systems and predict their structural properties. Particularly two series of Monte Carlo simulations are performed. The non-equilibrium case where we use varying temperatures and the equilibrium case where we test the affect of a single fixed temperature on the system. Results are displayed and explained extensively. The algorithms are implemented in Matlab language.

Contents

List of Figures

List of Tables

Chapter 1

Introduction

Recent observations of chiral structures in magnetic thin films have raised a great interest for the Dzyaloshinskii-Moriya interaction (DMI), as it favors magnetization rotations with a fixed chirality. This coupling originates from the combination of low structural symmetry and large spin-orbit coupling.

It has been first proposed in bulk materials lacking space inversion symmetry but it also exists at the interface between a magnetic film and a high spin-orbit coupling adjacent layer.The most striking phenomenon induced by DMI is the formation of skyrmion networks but its influence on domain walls is also at the origin of interesting properties such as increased domain wall velocity versus magnetic field. Recently, interest has also been devoted to isolated skyrmions, which can be nucleated as a metastable state in thin films opening a path to new concepts of magnetic memories based on skyrmion motion in nanotracks.

While extensive work has already been performed on the influence of DMI on micromagnetism for infinite samples, no description is available for nanostructures, which is the aim of the present work. We describe several cases with analytical solutions that provide tests for numerical codes, and help to get a physical feeling of the effects of this interaction.

Using simple physical arguments based on the micromagnetic length scales, we discuss the different states that are obtained. Current induced motion is under intensive study and it is a promising technique for the manipulation of magnetic information.

1.1 Magnetic Materials

1.1.1 Magnets

A magnet is a material or object that produces a magnetic field. This magnetic field is invisible but is responsible for the most notable property of a magnet: a force that pulls on other ferromagnetic materials, such as iron, and attracts or repels other magnets.

Materials that can be magnetized, which are also the ones that are strongly attracted to a magnet, are called ferromagnetic (or ferrimagnetic). These include iron, nickel, cobalt, some alloys of rare earth metals, and some naturally occurring minerals such as lodestone. Although ferromagnetic (and ferrimagnetic) materials are the only ones attracted to a magnet strongly enough to be commonly considered magnetic, all other substances respond weakly to a magnetic field, by one of several other types of magnetism.

Ferromagnetic materials can be divided into magnetically "soft" materials like annealed iron, which can be magnetized but do not tend to stay magnetized, and magnetically "hard" materials, which do. Permanent magnets are made from "hard" ferromagnetic materials such as alnico and ferrite

that are subjected to special processing in a powerful magnetic field during manufacture, to align their internal microcrystalline structure, making them very hard to demagnetize. To demagnetize a saturated magnet, a certain magnetic field must be applied, and this threshold depends on coercivity of the respective material. "Hard" materials have high coercivity, whereas "soft" materials have low coercivity.

The overall strength of a magnet is measured by its magnetic moment or, alternatively, the total magnetic flux it produces. The local strength of magnetism in a material is measured by its magnetization.

Magnetic field

The magnetic flux density, also called magnetic B field or just magnetic field, usually denoted B, is a vector field. The magnetic B field vector at a given point in space is specified by two properties:

1. Its direction, which is along the orientation of a compass needle.
2. Its magnitude,also called strength, which is proportional to how strongly the compass needle orients along that direction.

In SI units, the strength of the magnetic B field is given in teslas.

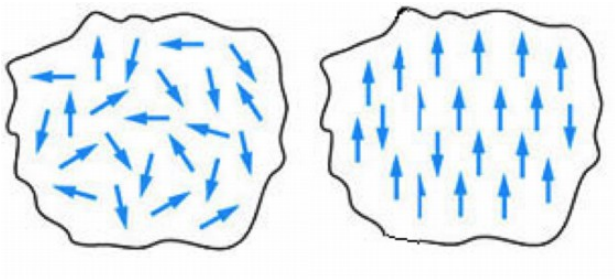

(a) Absence of Magnetic Field (b) Presence of Magnetic Field

Figure 1.1: Illustration of alignment of paramagnetic material in a magnetic field.

Magnetic moment

A magnet's magnetic moment,also called magnetic dipole moment and usually denoted μ, is a vector that characterizes the magnet's overall magnetic properties. For a bar magnet, the direction of the magnetic moment points from the magnet's south pole to its north pole, and the magnitude relates to how strong and how far apart these poles are. In SI units, the magnetic moment is specified in terms of $A \cdot m^2$ (amperes times meters squared).

A magnet both produces its own magnetic field and responds to magnetic fields. The strength of the magnetic field it produces is at any given point proportional to the magnitude of its magnetic moment. In addition, when the magnet is put into an external magnetic field, produced by a different source, it is subject to a torque tending to orient the magnetic moment parallel to the field. The amount of this torque is proportional both to the magnetic moment and the external field. A magnet may also be subject to a force driving it in one direction or another, according to the positions and orientations of the magnet and source. If the field is uniform in space, the magnet is subject to no net force, although it is subject to a torque.

Magnetization

The magnetization of a magnetized material is the local value of its magnetic moment per unit volume, usually denoted M, with units A/m.It is a vector field, rather than just a vector, like the magnetic moment, because different areas in a magnet can be magnetized with different directions and strengths. A good bar magnet may have a magnetic moment of magnitude $0.1A \cdot m^2$ and a volume of 1 cm^3, or $1 \times 10^{-6} m^3$, and therefore an average magnetization magnitude is 100,000 A/m. Iron can have a magnetization of around a million amperes per meter. Such a large value explains why iron magnets are so effective at producing magnetic fields.

1.1.2 Magnetism

Magnetism is a class of physical phenomena that are mediated by magnetic fields. Electric currents and the magnetic moments of elementary particles give rise to a magnetic field, which acts on other currents and magnetic moments. Every material is influenced to some extent by a magnetic field. The most familiar effect is on permanent magnets, which have persistent magnetic moments caused by ferromagnetism. The prefix ferro- refers to iron, because permanent magnetism was first observed in a form of natural iron ore called magnetite, Fe_3O_4. Most materials do not have permanent moments. Some are attracted to a magnetic field (paramagnetism); others are repulsed by a magnetic field (diamagnetism); others have a more complex relationship with an applied magnetic field (spin glass behavior and antiferromagnetism). Substances that are negligibly affected by magnetic fields are known as non-magnetic substances. These include copper, aluminium, gases, and plastic. Pure oxygen exhibits magnetic properties when cooled to a liquid state.

The magnetic state ,or magnetic phase, of a material depends on temperature and other variables such as pressure and the applied magnetic field. A material may exhibit more than one form of magnetism as these variables change.

Magnetism, at its root, arises from two sources:

1. Electric current.
2. Spin magnetic moments of elementary particles. The magnetic moments of the nuclei of atoms are typically thousands of times smaller than the electrons' magnetic moments, so they are negligible in the context of the magnetization of materials. Nuclear magnetic moments are very important in other contexts, particularly in nuclear magnetic resonance (NMR) and magnetic resonance imaging (MRI).

Ordinarily, the enormous number of electrons in a material are arranged such that their magnetic moments (both orbital and intrinsic) cancel out. This is due, to some extent, to electrons combining into pairs with opposite intrinsic magnetic moments as a result of the Pauli exclusion principle, or combining into filled subshells with zero net orbital motion. In both cases, the electron arrangement is so as to exactly cancel the magnetic moments from each electron. Moreover, even when the electron configuration is such that there are unpaired electrons and/or non-filled subshells, it is often the case that the various electrons in the solid will contribute magnetic moments that point in different, random directions, so that the material will not be magnetic.

However, sometimes,either spontaneously, or owing to an applied external magnetic field,each of the electron magnetic moments will be, on average, lined up. Then the material can produce a net total magnetic field, which can potentially be quite strong.

The magnetic behavior of a material depends on its structure, particularly its electron configuration, for the reasons mentioned above, and also on the temperature. At high temperatures, random thermal motion makes it more difficult for the electrons to maintain alignment.

The overall magnetic behavior of a material can vary widely, depending on the structure of the material, particularly on its electron configuration. Several forms of magnetic behavior have been observed in different materials, including:

Ferromagnetism

A ferromagnet, like a paramagnetic substance, has unpaired electrons. However, in addition to the electrons' intrinsic magnetic moment's tendency to be parallel to an applied field, there is also in these materials a tendency for these magnetic moments to orient parallel to each other to maintain a lowered-energy state. Thus, even in the absence of an applied field, the magnetic moments of the electrons in the material spontaneously line up parallel to one another.

Every ferromagnetic substance has its own individual temperature, called the Curie temperature, or Curie point, above which it loses its ferromagnetic properties. This is because the thermal tendency to disorder overwhelms the energy-lowering due to ferromagnetic order.

Ferromagnetism only occurs in a few substances; the common ones are iron, nickel, cobalt, their alloys, and some alloys of rare earth metals. The magnetic moments of atoms in a ferromagnetic material cause them to behave something like tiny permanent magnets. They stick together and align themselves into small regions of more or less uniform alignment called magnetic domains or Weiss domains. Magnetic domains can be observed with a magnetic force microscope to reveal magnetic domain boundaries. There are many scientific experiments that can physically show magnetic fields.

When a domain contains too many molecules, it becomes unstable and divides into two domains aligned in opposite directions so that they stick together more stably as shown at the right.

Figure 1.2: A domain wall in one dimension spin lattice indicated in red.

When exposed to a magnetic field, the domain boundaries move so that the domains aligned with the magnetic field grow and dominate the structure (dotted red area) as shown at the left. When the magnetizing field is removed, the domains may not return to an unmagnetized state. This results in the ferromagnetic material's being magnetized, forming a permanent magnet. When magnetized strongly enough that the prevailing domain overruns all others to result in only one single domain, the material is magnetically saturated. When a magnetized ferromagnetic material is heated to the Curie point temperature, the molecules are agitated to the point that the magnetic domains lose the organization and the magnetic properties they cause cease. When the material is cooled, this domain alignment structure spontaneously returns, in a manner roughly analogous to how a liquid can freeze into a crystalline solid.

Chapter 2

The Landau-Lifshitz equation

2.1 Magnetization vector

Suppose that all atoms in a specific material have a magnetic moment with the same magnitude, or that we can attribute to each lattice site in a solid material a magnetic moment with a certain constant magnitude. The magnetization properties of the material are defined by the atomic magnetic moments. In a ferromagnetic material the vector for the magnetic moment varies only slowly in space and it is then useful to treat the underlying material as a ferromagnetic continuum. That is, we may define the total magnetic moment in the unit volume of the material, or the density of magnetic moment M. We write approximately

$$M = \frac{\Delta\mu}{\Delta V}$$

where $\Delta\mu$ is the total magnetic moment in a volume element ΔV.The magnetization M has units A/m (Ampere per meter) in SI.

The magnetic moment density M is called the magnetization vector. As it gives the local density of the magnetic moments it is a function of position and maybe of time$M = M(r, t)$.As the magnetic moments of atoms are constant in magnitude the magnetization vector M is also considered to have a length which is constant in time. This is expressed by

$$M^2 = M_s^2$$

where M_s is called the saturation magnetization. The saturation magnetization can easily be measured when a magnetic sample is fully magnetized (saturated) along a certain direction (e.g.,by use of a strong magnetic field).

2.2 Magnetic energy

A ferromagnetic material is characterized by the property that neighbouring magnetic moments tend to be aligned with each other. For a chain of magnetic spins (moments) S_i an interaction which favours alignment of spins is typically expressed by the exchange interaction of the form

$$-J \sum_i S_i \cdot S_{i+1} \tag{2.1}$$

where J is the exchange constant. While this is the form of the exchange interaction for a discrete system of magnetic spins, these notes will only be concerned with a description of the continuum.

In order to derive a model for the continuum we first assume the magnetization vector M at discrete points α, β, etc, and treat them as classical vectors M_α, M_β.Assuming that α, β are neighboring sites we have the exchange contribution

$$-\frac{JS^2}{M_s^2} M_\alpha \cdot M_\beta$$

For a continuum model we may further assume that the magnetization vector varies slowly between neighboring sites. Let us take α, β to lie on the x-axis, with α the lattice spacing, and write

$$M_\beta \approx M_\alpha + \alpha \frac{\partial M_\alpha}{\partial x} + \frac{\alpha^2}{2} \frac{\partial^2 M_\alpha}{\partial x^2}$$

where the notation indicates that the derivatives are calculated at site α.For the neighbor of M_α on the opposite site we have a similar relation where $\alpha \to -\alpha$.Similar relations hold for the neighbors in the y, z directions. Thus the contribution to the exchange energy from the area of M_α is

$$-JS^2 \left[6 + \frac{\alpha^2}{M_s^2} M_\alpha \cdot \partial\mu \partial\mu M_\alpha \right]$$

where index μ takes values $\mu = 1, 2, 3$.

In a continuum form the term is described as The first term in the above form of the energy can be dropped as it is only a constant and by integrating over all space

$$E_{ex} = \frac{A}{M_s^2} \int \partial_\mu M \cdot \partial_\mu M d^3x \tag{2.2}$$

where index μ takes values $\mu = 1, 2, 3$.

We have introduced the exchange constant A which has units of J/m(Joule per meter), and the integration is extended over the volume of the magnetic material. The second form of the exchange energy is obtained from the first by a partial integration divergence theorem.

The main property of a ferromagnet which is implied by the exchange energy (2.2) is that the magnetization should tend to be uniform, or,$\partial_\mu M = 0$.On the other hand, the direction of the uniform magnetization is arbitrary, that is, the exchange energy term (2.2) is isotropic.

It is commonly seen that there are preferred directions in space for the orientation of magnetic moments, which depend on the crystal lattice of the material. We call this property the magnetocrystaline anisotropy or simply magnetic anisotropy. The simplest case is uniaxial magnetic anisotropy and it can be expressed by an energy term of the form

$$E_a = \frac{K}{M_s^2} \int (M_3)^2 d^3x \tag{2.3}$$

where K is the anisotropy constant in units of J/m^3 (Joule per $meter^3$).

If we assume $K > 0$, the energy term (2.3) disfavors the third component M_3 of the magnetization over the other two components (M_1, M_2). Such an energy term gives rise to easy-plane anisotropy, that is, the magnetization vector prefers to lie in the xy-plane. In the case $K < 0$ the M_3 component is favored and we would thus call the above an easy-axis anisotropy term.

Moreover, a third magnetic contribution is taken into account. The contribution to the total magnetic exchange interaction between two neighboring magnetic spins, S_i and S_j , also known as Dzyaloshinskii-Moriya interaction can be written as

$$H_{DM} = D_{ij} \cdot (S_i \times S_j)$$

Let us see how this discrete form is connected with the continuous form of the DM energy. If we express

$$\begin{aligned} S_{i,j} \times S_{i+1,j} \cdot \hat{e}_1 + S_{i-1,j} \times S_{i,j} \cdot \hat{e}_1 &= S_{i,j} \times (S_{i+1,j} - S_{i-1,j}) \cdot \hat{e}_1 \approx 2\Delta_x (m \times \partial_x m) \cdot \hat{e}_1 \\ S_{i,j} \times S_{i,j+1} \cdot \hat{e}_2 + Si, j-1 \times Si, j \cdot \hat{e}_2 &= S_{i,j} \times (S_{i,j+1} - S_{i,j-1}) \cdot \hat{e}_2 \approx 2\Delta_y (m \times \partial_y m) \cdot \hat{e}_2 \end{aligned}$$

then the Dzyaloshinskii-Moriya interaction energy term is

$$\begin{aligned} E_{DM} &\approx -\frac{D}{M_s^2} \sum \Delta_x (m \times \partial_x m) \cdot \hat{e}_1 + \Delta_y (m \times \partial_y m) \cdot \hat{e}_2 \\ &\approx -\frac{D}{M_s^2} \int (m_2 \partial_x m_3 - m_3 \partial_x m_2) + (m_3 \partial_y m_1 - m_1 \partial_y m_3) d^3x \\ &= \frac{D}{M_s^2} \int M \cdot (\nabla \times M) d^3x \end{aligned} \tag{2.4}$$

D is the continuous effective DMI constant, in J/m^2.

In magnetically ordered systems, it favors a spin canting of otherwise (anti)parallel aligned magnetic moments and thus, e.g., is a source of weak ferromagnetic behavior in an antiferromagnet.

The orientation of the vector D is constrained by symmetry. Considering the case that the magnetic interaction between two neighboring ions is transferred via a single third ion (ligand) by the superexchange mechanism, the orientation of D is obtained by the simple relation $D \propto r_i \times r_j = r_{ij} \times x$ (Fig.(2.1)).This implies that D is oriented perpendicular to the triangle spanned by the involved three ions. If the three ions are in line D = 0.

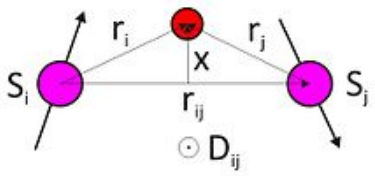

Figure 2.1: Determination of the orientation of the Dzyaloshinskii-Moriya vector from the local geometry.

Lastly, if the magnet is placed in an external magnetic field H_{ext} then this gives rise to the Zeeman energy term

$$E_{ext} = -\mu_0 \int H_{ext} \cdot M d^3x \tag{2.5}$$

Thus the total magnetic energy as the sum of exchange, anisotropy, Dzyaloshinskii-Moriya interaction, and external field energies is in the form [1],[2]

$$E = \frac{A}{M_s^2} \int \partial_\mu M \cdot \partial_\mu M d^3x + \frac{K}{M_s^2} \int (M_1^2 + M_2^2) d^3x + \frac{D}{M_s^2} \int M \cdot (\nabla \times M) d^3x - \mu_0 \int H_{ext} \cdot M d^3x \tag{2.6}$$

where x is the three-dimensional position vector.

2.3 Energy in rationalized units

For further calculations it will be very convenient to rationalize the expression for the energy[3]. First, M, as well as all quantities with the same units, are normalize to the saturation magnetization M_s so that $m^2 = 1$. Thus the rationalized fields are [1]

$$m \equiv \frac{M}{M_s}, \quad h_{ext} \equiv \frac{H_{ext}}{Ms} \tag{2.7}$$

We further use the exchange length $\ell_{ex} = \sqrt{2A/(\mu_0 M_s^2)}$ as the unit of length, hence the energy measured in units of $(\mu_0 M_s^2 \ell_{ex}^3)$ is given by

$$E = \frac{1}{2}\int \partial_i m \cdot \partial_i m \;\; d^3x + \frac{k_3}{2}\int (m_1^2 + m_2^2) d^3x + \lambda \int m \cdot (\nabla \times m) d^3x - \int h_{ext} \cdot m \;\; d^3x \tag{2.8}$$

where $k_3 \equiv 2K/(\mu_0 M_s^2)$ is the dimensionless anisotropy constant and

$$\lambda \equiv \frac{D}{\mu_0 M_s^2 \ell_{ex}}, \tag{2.9}$$

is the dimensionless Dzyaloshinskii-Moriya (DM) constant.

The parameter λ can be eliminated from the energy functional (2.8) if we use as a unit of length $\ell_D = \ell_{ex}/\lambda = 2A/D$ and redifine

$$k_3 = \frac{2K}{\mu_0 M_s^2} \cdot \frac{1}{\lambda^2} \tag{2.10}$$

Moreover the exchange term in the energy contains space derivatives, and therefore the ratio of the constant multiplying the exchange integral to, e.g., the constants of the anisotropy integral would produce a natural length scale for the system. This motivates the definition of the exchange length in Eq(2.9).

Substituting the definitions (2.7) in the energy (2.6) and measuring length in units of exchange length, we obtain the the energy of the system measured in units of so that the $(\mu_0 M_s^2 \ell_{ex}^3)$ in the form of Eq(2.8). The only constant remaining in the definition of the energy (2.8) is multiplying the anisotropy term and it is called the quality factor $k_3 = 2K/\mu_0 M_s^2$ and measures the strength of the anisotropy.

2.4 Landau-Lifshitz equation

A ferromagnetic medium is described in terms of the density of magnetic moment or magnetization M which is due primarily to the electron spin but may include contributions also from the orbital motion. In general, the vector $M = (M_1, M_2, M_3)$ is a function of position and time except that its magnitude is nearly constant for a wide temperature range sufficiently below the Curie point

$$M = M(x,t), \quad M^2 = M_1^2 + M_2^2 + M_3^2 = M_0^2$$

where $x = (x_1, x_2, x_3)$ is the position vector, t is the time variable and the constant M_0 is the saturation magnetization.

Static as well as dynamical properties of the magnetization are governed by the Landau-Lifshitz (LL) equation. Assume that the system is hamiltonian with an energy (2.8).To write Hamilton's equations as the equations of motion for the magnetization M ,we first note that the time derivatives of the canonical variables in the Hamiltonian formalism are given by the variation of $\delta E/\delta M$. The Landau-Lifshitz (LL) equation [4] is

$$\frac{\partial M}{\partial t} = -M \times F \tag{2.11}$$

which describes precession around an effective field F.

However, using all these constants within a theoretical development clouds the underlying simplicity of the Landau-Lifshitz equation. Hence we introduce rationalized physical units as described in Section(2.3). The (LL) equation (2.11) is then written as

$$\dot{M} + (M \times F) = 0 \tag{2.12}$$

At this moment a conserved energy function $E = E(M)$ exists such that the effective field is obtained through the general relation

$$F = -\frac{\delta E}{\delta M} \tag{2.13}$$

where the symbol δ denotes the usual functional derivative and F is given by

$$F = \Delta M - 2\lambda(\nabla \times M) + k_3 \hat{e}_3 m_3 + h_{ext}\hat{e}_3$$

Eq. (2.12) together wih Eq.(2.13) imply that the functional E is indeed conserved and that Eq.(2.11) is the Hamilton equation associated with the Hamiltonian E.

For a magnetic sample it is reasonable to assume that it may be uniformly magnetized along a certain direction as the exchange interaction tends to align all spins to each other. It is though evident that the direction of uniform magnetization is arbitrary if the magnet is isotropic. Let us consider the case of uniaxial anisotropy as in Eq. (2.3). Both orientations $\pm e_3$ are favored (when the z-axis is the easy direction of the magnetization) and thus there are two degenerate ground states for the system, namely the uniform magnetization states, $m = \pm(0, 0, 1)$. Note that in the Zeeman energy we will as well as subtract the (trivial) contribution from state $m = (0, 0, 1)$ which describes a fully saturated ferromagnet(ground state) that is the simplest example of a static solution of the (LL) equation.

All the above ensure that $E \geq 0$ and thus the minimum energy of the system is zero. Hence, one may assume $m = \pm(0, 0, 1)$ minimizes the total energy of the system (2.8).

2.5 Formulation with Angle variables

One may solve the constrain $m^2 = 1$ explicitly using,for example the spherical parametrization. As the magnetization is a vector with length $m^2 = 1$ it takes values on the unit sphere (S^2). Therefore it can be represented by two angles $0 \leq \Theta \leq \pi$ and $0 \leq \Phi \leq 2\pi$. The magnetization vector components are then given by the usual formula familiar from spherical coordinate transformations [1]

$$m_1 = \cos\Theta, \quad m_2 = \sin\Theta\cos\Phi, \quad m_3 = \sin\Theta\sin\Phi$$

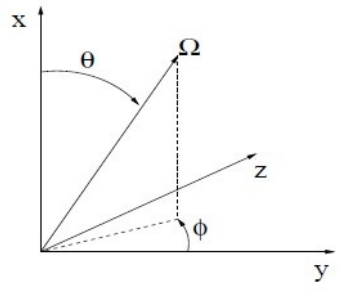

Figure 2.2: The coordinate system with angles Φ and Θ where $\Omega = (\cos\Theta, \sin\Theta\sin\Phi, \sin\Theta\cos\Phi)$.

We substitute the above form of the magnetization in the LL equation (2.13) and look for static solutions.

To calculate each term of the energy (2.8) we first calculate the derivatives

$$\begin{aligned}
\partial_i m_1 &= -\sin\Theta\partial_i\Theta \\
\partial_i m_2 &= \cos\Theta\cos\Phi\partial_i\Theta - \sin\Theta\sin\Phi\partial_i\Phi \\
\partial_i m_3 &= \cos\Theta\sin\Phi\partial_i\Theta + \sin\Theta\cos\Phi\partial_i\Phi
\end{aligned}$$

Then for the exchange term

$$\begin{aligned}\partial_i m \cdot \partial_i m &= (-\sin\Theta\partial_i\Theta)^2 + (\cos\Theta\cos\Phi\partial_i\Theta - \sin\Theta\sin\Phi\partial_i\Phi)^2 + (\cos\Theta\sin\Phi\partial_i\Theta + \sin\Theta\cos\Phi\partial_i\Phi)^2 \\ &= \sin^2\Theta\partial_i^2\Theta + \cos^2\Theta\cos^2\Phi\partial_i^2\Theta - 2\cos\Theta\cos\Phi\partial_i\Theta\sin\Theta\sin\Phi\partial_i\Phi + \sin^2\Theta\sin^2\Phi\partial_i^2\Phi + \\ &\quad \cos^2\Theta\sin^2\Phi\partial_i^2\Theta + 2\cos\Theta\cos\Phi\partial_i\Theta\sin\Theta\sin\Phi\partial_i\Phi + \sin^2\Theta\cos^2\Phi\partial_i^2\Phi \\ &= \partial_i\Theta\cdot\partial_i\Theta + \sin^2\Theta\partial_i^2\Phi\end{aligned}$$

Therefore, the exchange energy term becomes

$$E_{ex} = \frac{1}{2}\int \partial_i m \cdot \partial_i m \;\; d^3x = \frac{1}{2}\int (\partial_i\Theta\cdot\partial_i\Theta + \sin^2\Theta\partial_i^2\Phi)d^3x \tag{2.14}$$

The DM term can be written more explicitly as

$$\begin{aligned}m\cdot(\nabla\times m) &= m_1(\partial_2 m_3 - \partial_3 m_2) + m_2(\partial_3 m_1 - \partial_1 m_3) + m_3(\partial_1 m_2 - \partial_2 m_1) \\ &= \cos\Theta(\cos\Theta\sin\Phi\partial_2\Theta + \sin\Theta\cos\Phi\partial_2\Phi - \cos\Theta\cos\Phi\partial_3\Theta - \sin\Theta\sin\Phi\partial_3\Phi) \\ &\quad + \sin\Theta\cos\Phi(-\sin\Theta\partial_3\Theta - \cos\Theta\sin\Phi\partial_1\Theta - \sin\Theta\cos\Phi\partial_1\Phi) \\ &\quad + \sin\Theta\cos\Phi(\cos\Theta\cos\Phi\partial_1\Theta - \sin\Theta\sin\Phi\partial_1\Phi + \sin\Theta\partial_2\Theta) \\ &= \cos^2\Theta\sin\Phi\partial_2\Theta + \sin\Theta\cos^2\Theta\cos\Phi\partial_2\Phi - \cos\Theta\cos\Phi\partial_3\Theta - \cos\Theta\sin\Theta\sin\Phi\partial_3\Phi \\ &\quad - \cos\Phi\sin^2\Theta\partial_3\Theta - \cos\Theta\cos\Phi\sin\Theta\sin\Phi\partial_1\Theta - \sin^2\Theta\cos^2\Phi\partial_1\Phi \\ &\quad + \cos\Theta\cos\Phi\sin\Phi\sin\Theta\partial_1\Theta + \sin^2\Theta\sin\Phi\partial_2\Theta - \sin^2\Phi\sin^2\Phi\partial_1\Theta \\ &= -\sin^2\Theta\partial_1\Phi + \sin\Phi\partial_2\Theta - \cos^2\Phi\partial_3\Theta + \cos\Theta\sin\Theta(\cos\Phi\partial_2\Phi + \sin\Phi\partial_3\Phi)\end{aligned}$$

Thus, the DM interaction energy term is

$$\begin{aligned}E_{DM} &= \lambda\int m\cdot(\nabla\times m)dx \\ &= \lambda\Big[\int -\sin^2\Theta\partial_1\Phi + \sin\Phi\partial_2\Theta - \cos^2\Phi\partial_3\Theta \\ &+ \;\; \cos\Theta\sin\Theta(\cos\Phi\partial_2\Phi + \sin\Phi\partial_3\Phi)d^3x\Big]\end{aligned} \tag{2.15}$$

Without loss of generality, we will let the uniform magnetic field of strength h_{ext} as well as anisotropy,to point along the third axis(easy-axis).Then the anisotropy term becomes

$$E_a = \frac{k_3}{2}\int (m_1^2 + m_2^2)d^3x = \frac{k_3}{2}\int (1 - m_3^2)d^3x = \frac{k_3}{2}\int (1 - \sin^2\Theta\sin^2\Phi) \;\; d^3x \tag{2.16}$$

where $m^2 = m_1^2 + m_2^2 + m_3^2 = 1$.

Lastly, the external magnetic field term is

$$E_{ext} = h_{ext}\int (1 - m_3)d^3x = h_{ext}\int (1 - \sin\Theta\sin\Phi)dx \tag{2.17}$$

Hence the final energy functional is parametrized in terms of the two independent fields Θ and Φ and reads

$$\begin{aligned}E = \int \Big[\frac{1}{2}(\partial_i^2\Theta + \sin^2\Theta\partial_i^2\Phi) + \lambda[-\sin^2\Theta\partial_1\Phi + \sin\Phi\partial_2\Theta - \cos^2\Phi\partial_3\Theta + \cos\Theta\sin\Theta(\cos\Phi\partial_2\Phi + \sin\Phi\partial_3\Phi)] \\ + \frac{k_3}{2}(1 - \sin^2\Theta\sin^2\Phi) + h_{ext}(1 - \sin\Theta\sin\Phi)\Big]d^3x\end{aligned} \tag{2.18}$$

The variational derivatives of Eq.(2.13), using Calculus of Variations, are of the form

$$\begin{aligned}\frac{\delta E}{\delta \Phi} &= -\partial_i \Phi(sin^2\Theta\partial_i\Phi) + \lambda[sin^2\Theta\partial_1\Phi + 2sin^2\Theta(cos\Phi\partial_2\Theta + sin\Phi\partial_3\Theta)] - k_3\cos\Phi\sin\Phi\sin^2\Theta \\ &\quad -h_{ext}\sin\Theta\cos\Phi \qquad (2.19)\\ \frac{\delta E}{\delta \Theta} &= -\partial_i\Theta + cos\Theta sin\Theta[(\partial_i^2\Phi) - 2\lambda\partial_1\Phi] - 2\lambda sin^2\Theta(\sin\Phi\partial_2\Phi - \cos\Phi\partial_3\Phi) - k_3\cos\Theta\sin\Theta\sin^2\Phi \\ &\quad -h_{ext}\cos\Theta\sin\Phi \qquad (2.20)\end{aligned}$$

Chapter 3

Domain Wall and Spiral solutions

From now on in this thesis we will deal with the one dimension case of the problem.

Assume that the system is spiral along x and $\Theta = \Theta(x)$, $\Phi = \Phi(x)$ then Eq.(2.19),(2.20) yields

$$\frac{\delta E}{\delta \Phi} = -(\sin^2\Theta\Phi')' + \lambda(\sin^2\Theta)' - k_3\cos\Phi\sin\Phi\sin^2\Theta - h_{ext}\sin\Theta\cos\Phi \tag{3.1}$$

$$\frac{\delta E}{\delta \Theta} = -\Theta'' + \cos\Theta\sin\Theta(\Phi'^2 - 2\lambda\Phi') - k_3\cos\Theta\sin\Theta\sin^2\Phi - h_{ext}\cos\Theta\sin\Phi \tag{3.2}$$

and the corresponding energy functional in Eq.(2.18) becomes

$$E = \int \left[\frac{1}{2}(\Theta'^2 + \sin^2\Theta\Phi'^2) - \lambda\sin^2\Theta\Phi' + \frac{k_3}{2}(1 - \sin^2\Theta\sin^2\Phi) + h_{est}(1 - \sin\Theta\sin\Phi)\right]dx \tag{3.3}$$

The static equations are

$$\frac{\delta E}{\delta \Phi} = \frac{\delta E}{\delta \Theta} = 0$$

and we may further assume that $\Theta = \pi/2$ so that the second equation $\delta E/\delta\Theta = 0$ is automatically satisfied. The value of angle Θ could be for example 0,π or $\pi/2$. The choice of $\Theta = \pi/2$ is so that we obtain the simplest differential equation governed from the static equations. For $\Theta = 0$ or π it is clear that both static equations are zero.

Then Eq.(3.1) yields

$$-\Phi'' - h\sin\Phi - k_3\cos\Phi\sin\Phi = 0 \tag{3.4}$$

In a finite dimension structure with DMI, the uniform state $m = (0, 0, \pm 1)$ is never a solution of the micromagnetic problem as soon as $\lambda \neq 0$. What is clear in Eq.(3.4) is that there is absence of the DMI term. That is to say that the uniform state could be as solution to the problem. It is also interesting to note that DMI does not change the shape of the 1D domain wall but introduces chirality, of a sign fixed by that of λ. For the most favorable chirality, it lowers the energy.

The energy functional here is

$$E = \int \left[\frac{1}{2}\Phi'^2 - \lambda\Phi' + \frac{k_3}{2}\cos^2\Phi + h_{est}(1 - \cos\Phi)\right]dx \tag{3.5}$$

In the following Chapters all calculations will be performed for the one dimensional case where the temperature of the system is zero in all of the cases.

3.1 Domain Wall

For a system with two degenerate ground states it is possible that different regions of the sample may be in one or in the other ground state. Regions with uniform magnetization are called magnetic domains. To define the magnetization suppose that we have two domains which are magnetized along the z-axis while they are located at $x > 0$ and $x < 0$ respectively (they are separated by the yz-plane). Landau and Lifshitz have proposed that the magnetization rotates gradually in the yz-plane as we move from one domain to the other along the x-axis.

In the absence of DM interaction and external field the the Eq.(3.4) is

$$-\Phi'' - k_3 \cos\Phi \sin\Phi = 0 \Leftrightarrow \Phi'' = -\frac{\cos\Phi \sin\Phi}{\Delta^2} \quad \text{where} \quad \Delta = \frac{1}{\sqrt{k_3}} \tag{3.6}$$

Then we integrate Eq.(3.6) over x to obtain an equation for Φ

$$\Delta^2 \Phi'^2 = \cos^2\Phi + C, \quad \text{where } C \textit{ is some integration constant} \tag{3.7}$$

There are 4 trivial solutions, $\Phi(x) = 0, \pi/2, \pi$, and $3\pi/2$, which are uniform. However, only 0 and π are stable (the anisotropy energy density is zero)[5].

The constant can be determined by noting that for a domain-wall, $\partial_x \Phi(\pm\infty) = 0$,so that $\Phi(x)$ cannot diverge, and $\Phi(\pm\infty) = (0, \pi)$.Therefore the integration constant is $C = 0$.

The square root of Eq.(3.7) is

$$\Phi' = \pm\frac{\cos\Phi}{\Delta} \Leftrightarrow \frac{d\Phi}{\cos\Phi} = \pm\frac{1}{\Delta}dx \tag{3.8}$$

We use the variable $t = \tan(\Phi/2)$ and remark that $\cos\Phi = (1-t^2)/(1+t^2)$ and the Eq.(3.8) becomes

$$\frac{dt}{t} = \pm\frac{dx}{\Delta} \Leftrightarrow ln(t) = \pm\frac{x}{\Delta} \Leftrightarrow ln(\tan(\Phi/2)) = \pm\frac{x}{\Delta}$$

which has the domain wall solution

$$\Phi(x) = 2arctan\left(e^{(\pm x/\Delta)}\right) \quad \text{where} \quad \Delta = \frac{1}{\sqrt{k_3}} \tag{3.9}$$

This solution corresponds to a domain wall solution. Given the singe + or - the magnetization turns from $\Phi = 0$ to π (+ sign) or from π to 0. All these solutions are equivalent. The Bloch wall parameter Δ is proportional to the domain wall width. It corresponds to one of the characteristic length in micro-magnetism, which compares the magnetic anisotropy strength with the exchange energy. It is easily seen that higher anisotropy energy favors narrower domain walls.

The $\pm$ sign is fully determined by the derivative of Φ, which corresponds to going from $\Phi = 0$ on the left to $\Phi = \pi$ on the right, or vice-versa. This freedom is called the topological charge Q of the domain-wall. A positive or negative topological charge (Q=+1 or Q=-1) corresponds to a domain-wall going from $\pm z$ on the left to $\mp z$ on the right. Therefore, a positive charge corresponds to $\partial_x \Phi > 0$, and a negative charge corresponds to $\partial_x \Phi < 0$. The name "charge" comes from the fact that it determines the way in which an external field affects the domain-wall. With positive charge and an external magnetic field in the $+z$ direction, the domain-wall will move in the $+x$ direction [6].

There is one more freedom, that comes from the angle Φ. Remember that in order to have a domain-wall in the easy-plane, we had to choose $\Phi = 0$ or $\Phi = \pi$. This choice determines the direction of the spin in the center of the domain-wall. Associated with this freedom is the so-called chirality C.

A positive chirality (C=+1) corresponds to a clockwise rotation of the spins from the left to the right and a negative chirality (C=-1) to a counter-clockwise rotation. The combination of charge Q and chirality C yields a total of four Bloch wall configurations, as shown in Fig.(3.1).

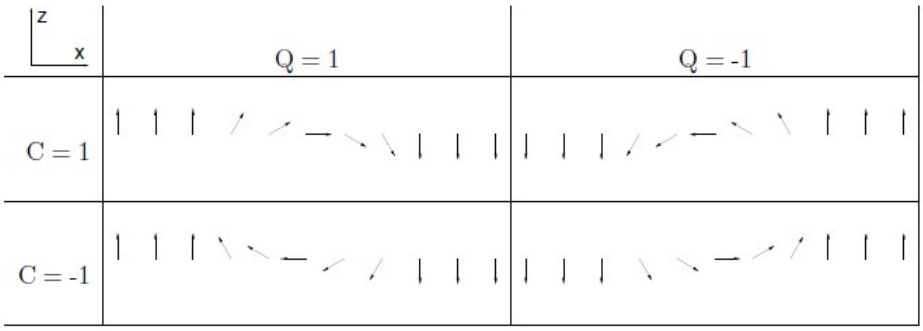

Figure 3.1: The four Bloch wall configurations.

Let us now calculate the energy of the domain wall.

$$\begin{aligned} E &= \int_{-\infty}^{+\infty}\left[\frac{1}{2}\left(\frac{\partial\Phi}{\partial x}\right)^2+\frac{k_3}{2}\cos^2\Phi\right]dx=\int_{-\infty}^{+\infty}\left[\frac{1}{2\Delta^2}\cos^2\Phi+\frac{1}{2\Delta^2}\cos^2\Phi\right]dx \\ &= \frac{1}{\Delta^2}\int_{-\infty}^{+\infty}\cos^2\Phi dx=\frac{1}{\Delta^2}\int_{-\infty}^{+\infty}\cos^2\left(2arctan(e^{(\pm x/\Delta)})\right)dx=\frac{1}{\Delta^2}\int_{-\infty}^{+\infty}\frac{4e^{2x/\Delta}}{(e^{2x/\Delta}+1)^2} \\ &= \frac{1}{\Delta^2}\left[\lim_{B\to-\infty}\int_B^a\frac{4e^{2x/\Delta}}{(e^{2x/\Delta}+1)^2}+\lim_{B\to+\infty}\int_a^B\frac{4e^{2x/\Delta}}{(e^{2x/\Delta}+1)^2}\right]=\frac{2\cdot\Delta}{\Delta^2}=2\sqrt{k_3}>0 \end{aligned} \tag{3.10}$$

The corresponding magnetization is

$$m_1=0,\quad m_2=\frac{2e^{\pm x/\Delta}}{e^{\pm 2\Delta x}+1},\quad m_3=-\frac{e^{\pm 2\Delta x}-1}{e^{\pm 2\Delta x}+1},\quad \text{where}\quad \Delta=\frac{1}{\sqrt{k_3}}.$$

Using the following trigonometric identities

$$tanh(x)=\frac{e^{2x}-1}{e^{2x}+1},\quad cosh(x)=\frac{e^x+e^{-x}}{2}$$

the magnetization becomes [5]

$$m_1=0,\quad m_2=\pm\frac{1}{\cosh\left(x/\Delta\right)},\quad m_3=\pm\tanh\left(x/\Delta\right)\quad \text{where}\quad \Delta=\frac{1}{\sqrt{k_3}}. \tag{3.11}$$

The representation of the magnetization in this case is shown in Fig.(3.2). We should denote that the domain wall lies between the transition of the positive to the negative domain and vice-versa.

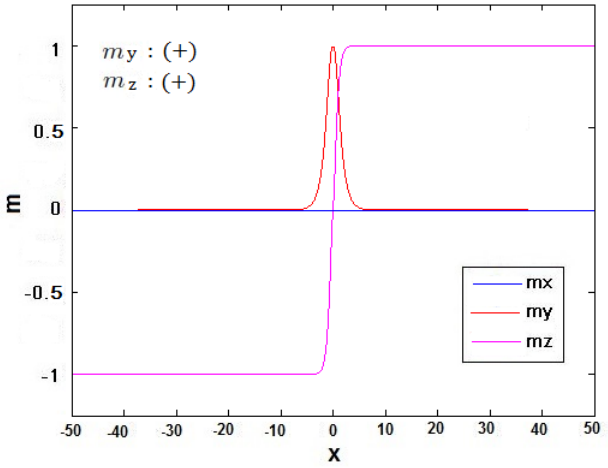

(a)

Figure 3.2: Magnetization of a domain wall solution at T=0.

3.2 Dzyaloshinskii-Moriya interaction and Anisotropy

In the absence of easy-axis anisotropy, where that is to say that $k_3 = 0$,the system becomes

$$\Phi'' = 0$$

Assume that we have the boundary condition $\partial_x \Phi = \lambda$. We may then choose the solution $\Phi = \lambda x$. So, the magnetisation for $\Theta = \pi/2$ is

$$m_1 = 0, \quad m_2 = \cos(\lambda x), \quad m_3 = \sin(\lambda x) \tag{3.12}$$

and it is called spiral. The period of the spiral is $2\pi/\lambda$.

The graph of the magnetization for $\lambda = 1$ is shown in Fig.(3.3). The period of the spiral solution here is 2π.

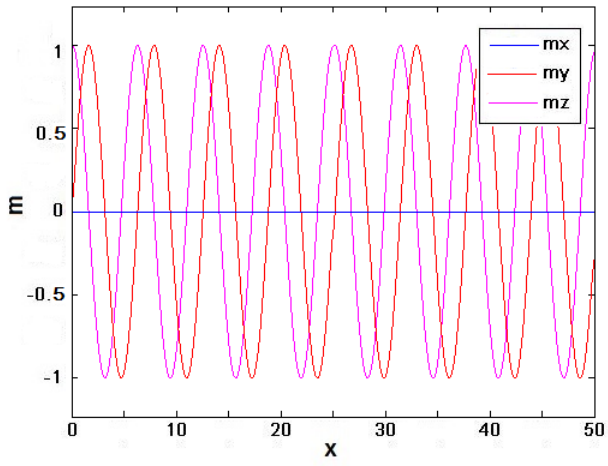

(a)

Figure 3.3: Magnetization of a spiral solution at T=0.

In this case we may assume that the system is a periodic proliferation of domain walls. Hence it would

be wise to calculate the average energy density over a period L. That is

$$\begin{aligned}\mathcal{E} &= \frac{1}{L}\int_{-\frac{L}{2}}^{\frac{L}{2}}\left[\frac{1}{2}\left(\frac{\partial\Phi}{\partial x}\right)^2-\lambda\frac{\partial\Phi}{\partial x}\right]dx=\frac{1}{L}\int_{-\frac{L}{2}}^{\frac{L}{2}}\left(\frac{\lambda^2}{2}-\lambda^2\right)dx\\ &= -\frac{1}{L}\frac{\lambda^2}{2}\int_{-\frac{L}{2}}^{\frac{L}{2}}dx=-\frac{1}{L}\frac{\lambda^2}{2}\left[\frac{L}{2}+\frac{L}{2}\right]=-\frac{\lambda^2}{2}\end{aligned} \tag{3.13}$$

Adding Dzyaloshinskii-Moriya interaction to the system (3.4) we obtain once again the Eq.(3.6) which ,as we have already proved, has the solution (3.9). Correspondingly the magnetization is of the form (3.11).

Despite the fact that the solution of the system is also a domain wall solution the energy functional is of the form

$$\begin{aligned}E &= \int_{-\infty}^{+\infty}\left[\frac{1}{2}\left(\frac{\partial\Phi}{\partial x}\right)^2-\lambda\frac{\partial\Phi}{\partial x}+\frac{k_3}{2}\cos^2\Phi\right]dx=\int_{-\infty}^{+\infty}\left[\frac{1}{2}\left(\frac{\partial\Phi}{\partial x}\right)^2+\frac{k_3}{2}\cos^2\Phi\right]dx\pm\lambda\int_{-\infty}^{+\infty}\frac{\partial\Phi}{\partial x}dx\\ &= 2\sqrt{k_3}\pm\lambda\int_{-\infty}^{+\infty}\frac{1}{\Delta}\cos\Phi dx=2\sqrt{k_3}\pm\lambda\frac{1}{\Delta}\int_{-\infty}^{+\infty}\cos\Phi dx=2\sqrt{k_3}\pm\frac{\lambda}{\Delta}\int_{-\infty}^{+\infty}\cos\left(2arctan(e^{(\pm x/\Delta)})\right)dx\\ &= 2\sqrt{k_3}\pm\frac{\lambda}{\Delta}\int_{-\infty}^{+\infty}\frac{1-e^{(\pm 2x/\Delta)}}{e^{(\pm 2x/\Delta)}+1}dx=2\sqrt{k_3}\pm\frac{\lambda}{\Delta}\Delta\pi=2\sqrt{k_3}\pm\lambda\pi\end{aligned} \tag{3.14}$$

The $\pm$ sign on the energy indicates that the DMI term does not change the shape of the 1D domain wall but introduces chirality, of a sign fixed by that of λ. For the most favorable chirality, it lowers the energy.

One may observe that $E\leq 0$ if [1]

$$2\sqrt{k_3}\pm\lambda\pi\leq 0\Leftrightarrow\sqrt{k_3}\leq\pm\frac{\lambda\pi}{2}\Leftrightarrow k_3\leq\frac{\pi^2}{4}\lambda^2 \tag{3.15}$$

This leads to the conclusion that when a domain wall is inserted in the system ,the energy is reduced below the energy of the ferromagnetic state. We may then conjecture a proliferation of domain walls for $k_3\leq\pi^2\lambda^2/4$.

3.3 Spiral in the presence of External field

In this case where there is total absence of anisotropy the Eq.(3.4) becomes

$$-\Phi''-h\cos\Phi=0\Leftrightarrow\Phi''+h\cos\Phi=0\Leftrightarrow\Phi'^2+2h\sin\Phi=C$$

Integrating over x and for $C=\delta^2+2h$

$$\Phi'^2+2h\sin\Phi=\delta^2+2h\Leftrightarrow\Phi'^2=2h(1-\sin\Phi)+\delta^2\Leftrightarrow\Phi'=\sqrt{2h(1-\sin\Phi)+\delta^2} \tag{3.16}$$

The solution of (3.16) is given by the implicit equation

$$\frac{d\Phi}{dx}=\sqrt{2h(1-\sin\Phi)+\delta^2}\Leftrightarrow dx=\frac{d\Phi}{\sqrt{2h(1-\sin\Phi)+\delta^2}}\Leftrightarrow\int_0^X d\tilde{x}=\int_0^\Phi\frac{d\phi}{\sqrt{2h(1-\sin\Phi)+\delta^2}}\Leftrightarrow$$

$$X=\int_0^\Phi\frac{d\phi}{\sqrt{2h(1-\sin\Phi)+\delta^2}} \tag{3.17}$$

a periodic function $\Phi = \Phi(x)$ with period

$$L = \int_0^{2\pi} \frac{d\phi}{\sqrt{\delta^2 + 2h(1-\sin\phi)}} \tag{3.18}$$

The average energy density defined from

$$\mathcal{E} = \frac{1}{L}\int_0^L \left[\frac{1}{2}\Phi'^2 - \lambda\Phi' + h_{ext}(1-\sin\Phi)\right]dx$$

is optimized with respect to δ^2 to yield an algebraic equation for δ^2:

$$\frac{1}{2\pi}\int_0^{2\pi} \sqrt{\delta^2 + 2h_{ext}(1-\sin\Phi)}d\Phi = \lambda, \quad \mathcal{E} = -\frac{\delta^2}{2} \tag{3.19}$$

Critical field from the above equation with $\delta = 0$ is

$$J_c = \frac{1}{2\pi}\int_0^{2\pi} \sqrt{1-\sin\Phi}d\Phi = 0.9, \quad h_c = \frac{\lambda^2}{2J^2} = \frac{\pi^2}{16}\lambda^2, \tag{3.20}$$

Chapter 4

Metropolis Monte Carlo algorithm

4.1 Monte Carlo methods

Monte Carlo methods (or Monte Carlo experiments) are a broad class of computational algorithms that rely on repeated random sampling to obtain numerical results. They are often used in physical and mathematical problems and are most useful when it is difficult or impossible to use other mathematical methods. Monte Carlo methods are mainly used in three distinct problem classes: optimization, numerical integration, and generating draws from a probability distribution.

In principle, Monte Carlo methods can be used to solve any problem having a probabilistic interpretation. By the law of large numbers, integrals described by the expected value of some random variable can be approximated by taking the empirical mean (a.k.a. the sample mean) of independent samples of the variable. When the probability distribution of the variable is parameterized, mathematicians often use a Markov Chain Monte Carlo (MCMC) sampler [7]. The central idea is to design a judicious Markov chain model with a prescribed stationary probability distribution. By the ergodic theorem, the stationary distribution is approximated by the empirical measures of the random states of the MCMC sampler.

A Markov chain is said to be ergodic if the probabilities of transitioning between states are such that any state can eventually transition to any other state. A powerful theorem known as the $Perron - Frobenius$ theorem asserts that for ergodic Markov chains there is a unique probability distribution which is invariant under the transition rules. That is, there is a unique equilibrium distribution. The transition probabilities, $P(x'|x)$ describe the probability of transitioning from any given state, x, to any other given state, x'. Then the Markov process has a unique stationary distribution $\pi(x)$ when the following two conditions are met:[8]

1 There must exist a stationary distribution $\pi(x)$. A sufficient but not necessary condition is detailed balance which requires that each transition $x \longrightarrow x'$ is reversible: for every pair of states x, x', the probability of being in state x and transitioning to state x' must be equal to the probability of being in state x' and transitioning to state x, $\pi(x)P(x'|x) = \pi(x')P(x|x')$.

2 The stationary distribution $\pi(x)$ must be unique. This is guaranteed by ergodicity of the Markov process, which requires that every state must (1) be aperiodic,the system does not return to the same state at fixed intervals and (2) be positive recurrent,the expected number of steps for returning to the same state is finite.

Uses of Monte Carlo methods require large amounts of random numbers, and it was their use that spurred the development of pseudorandom number generators, which were far quicker to use than the tables of random numbers that had been previously used for statistical sampling.Pseudo-random number sampling algorithms are used to transform uniformly distributed pseudo-random numbers into numbers that are distributed according to a given probability distribution.

Moreover, in Monte Carlo simulation, the entire system is simulated a large number of times. Each simulation is equally likely, referred to as a realization of the system. For each realization, all of the uncertain parameters are sampled (i.e., a single random value is selected from the specified distribution describing each parameter). The system is then simulated through time,given the particular set of input parameters, such that the performance of the system can be computed. This is a large number of separate and independent results,one possible path the system may follow through time. Those results of the independent system realizations are assembled into probability distributions of possible outcomes. Thus, the outputs are not single values, but probability distributions.

4.1.1 Metropolis–Hastings algorithm

Metropolis–Hastings algorithm is a Markov chain Monte Carlo (MCMC) method for obtaining a sequence of random samples from a probability distribution for which direct sampling is difficult. The algorithm can draw samples from any probability distribution $P(x)$, provided you can compute the value of a function $f(x)$ which is proportional to the density of P. The lax requirement that $f(x)$ should be merely proportional to the density.

The Metropolis–Hastings algorithm generates a sequence of sample values that are produced iteratively with the distribution of the next sample being dependent only on the current sample value. As more sample values are produced, the distribution of those values more closely approximates the desired distribution $P(x)$, making the sample sequence into a Markov chain.

Specifically, at each iteration, the algorithm picks a candidate for the next sample value based on the current sample value. Then, with some probability, the candidate is either accepted or rejected. In the first case, the candidate value is used in the next iteration. On the contrary, in the second case,the candidate value is discarded, and current value is reused in the next iteration. The probability of acceptance is determined by comparing the values of the function $f(x)$ of the current and candidate sample values with respect to the desired distribution $P(x)$.

4.1.2 Metropolis Monte Carlo algorithm

Metropolis Monte Carlo algorithm is a special case of the Metropolis–Hastings algorithm where the proposal function P is symmetric. In other words, it must satisfy $P(x|y) = P(y|x)$. It is accomplished by first making a random move, then evaluating the Boltzmann probability of that move and comparing the probability against a random number. The Boltzmann distribution describes the probability of a system to be in a certain state as a function of that state's energy and temperature. It is given as

$$P_i = \frac{e^{-\beta H_i}}{\sum_{j=1}^{M} e^{-\beta H_j}} = \frac{1}{Z} e^{-\beta H_i}$$

where P_i is the probability of state i,H_i is the energy of state i ,$\beta = \frac{1}{kT}$ where k is the Boltzmann constant and T is the temperature of the system and M is the number of energy states accessible to the system. The variable Z is the sum over all the possible energy states M that is called partition function.

If the Boltzmann probability of the move is larger than the random number, the move is accepted. Otherwise, the system is returned to its original configuration. At the end, a set of configurations is obtained according to Boltzmann statistics and the expectation value of a property is obtained as a simple arithmetic average of property values from individual accepted configurations.

The algorithm first chooses selection probabilities $g(\mu, \nu)$, which represent the probability that state ν is selected by the algorithm out of all states, given that we are in state μ. It then uses acceptance probabilities $A(\mu, \nu)$ so that detailed balance is satisfied. If the new state ν is accepted, then we move

to that state and repeat with selecting a new state and deciding to accept it. If ν is not accepted then we stay in μ. When implementing the algorithm, we must ensure that $g(\mu, \nu)$ is selected such that ergodicity is met. The energy of the present state is written as $H\mu$ and correspondingly the energy of any other possible new state is written as $H\nu$.

Detailed balance [8] requires that the following equation must hold

$$\frac{P(\mu,\nu)}{P(\nu,\mu)} = \frac{g(\mu,\nu)A(\mu,\nu)}{g(\nu,\mu)A(\nu,\mu)} = \frac{A(\mu,\nu)}{A(\nu,\mu)} = \frac{P_\beta(\nu)}{P_\beta(\mu)} = \frac{\frac{1}{Z}e^{-\beta(H\nu)}}{\frac{1}{Z}e^{-\beta(H\mu)}} = e^{-\beta(H_{\nu\mu})} \quad \text{where} \quad H_{\nu\mu} = H_\nu - H_\mu$$

Thus, we want to select the acceptance probability for our algorithm to satisfy

$$\frac{A(\mu,\nu)}{A(\nu,\mu)} = e^{-\beta(H_{\nu\mu})}$$

The acceptance probability for $H_\nu > H_\mu$ is

$$A(\mu,\nu) = \begin{cases} e^{-\beta(H_{\nu\mu})}, & \text{if } H_\nu - H_\mu > 0 \\ 1, & \text{otherwise} \end{cases}$$

Algorithm Implementation

Algorithm 1 Metropolis Monte Carlo algorithm

```
procedure GENERATES A NEW CONFIGURATION FROM A PREVIOUS ONE SO THAT THE TRANSITION PROBABILITY SATISFIES THE DETAILED BALANCE CONDITION
    Choose the initial configuration of the system
    Calculate the energy
    for each particle i ∈ N do
        Pick a random displacement d ∈ (0, 1) for x, y and z coordinates
        Calculate the energy change ΔH due to the displacement
        if ΔH<0 then
            accept the new configuration
        else
            calculate A = exp(−ΔH/kT)
            Draw a random number r ∈ (0, 1)
            if A>r then
                accept the new configuration
            else
                keep the old one
            end if
        end if
    end for
end procedure
```

4.2 Lattice Monte Carlo

Monte Carlo simulations on a lattice provide a faster alternative to continuum Monte Carlo methods and Molecular Dynamics, but are generally less accurate. Models in which particles belong to the

lattice sites and interact locally can be a good representation of a number of real systems (magnetic materials, binary alloys, etc.). There are several modifications of lattice MC such as the Heisenberg Model.

4.2.1 Heisenberg Model

The Heisenberg model is a statistical mechanical model used in the study of critical points and phase transitions of magnetic systems, in which the spins of the magnetic systems are treated quantum mechanically. In the prototypical Ising model, defined on a d-dimensional lattice, at each lattice site, a spin $\sigma_i \in \{\pm 1\}$ represents a microscopic magnetic dipole to which the magnetic moment is either up or down. Except the coupling between magnetic dipole moments, there is also a multipolar version of Heisenberg model called the multipolar exchange interaction.

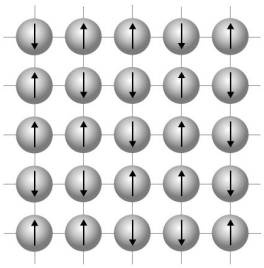

Figure 4.1: An Heisenberg Model.

For quantum mechanical reasons the dominant coupling between two dipoles may cause nearest-neighbors to have lowest energy when they are aligned. Under this assumption,so that magnetic interactions only occur between adjacent dipoles, the Hamiltonian can be written in the form

$$\hat{H} = -J \sum_{j=1}^{N} \sigma_j \sigma_{j+1} - h \sum_{j=1}^{N} \sigma_j$$

where J is the coupling constant for a 1-dimensional model consisting of N dipoles, represented by classical vectors (or spins) σ_j, subject to the periodic boundary condition $\sigma_{N+1} = \sigma_1$.

4.2.2 Classical Heisenberg model

The Classical Heisenberg model is the n=3 case of the n-vector model [9] used mainly in statistical physics to model ferromagnetism.

Classical Heisenberg Model simulation

It is easy to view the Heisenberg Model as a Markov Chain, as the immediate future state ν transition probability $P_\beta(\nu)$ only depends on the present state μ. This motivates the reason for the Heisenberg Model to be simulated using Monte Carlo Methods and especially with Metropolis Monte Carlo algorithm . Specifically, Metropolis MC algorithm requires ergodicity to be implemented. This is the motivation behind the concept of single-spin-flip dynamics , which states that in each transition, we will only change one of the spin sites on the lattice. Furthermore, by using single- spin-flip dynamics, we can get from any state to any other state by flipping each site that differs between the two states one at a time.

To simulate this model we can take a d-dimensional lattice, and a set of spins of the unit length

$$\vec{s_i} \in \mathbb{R}^3, |\vec{s_i}| = 1$$

each one placed on a lattice node. The model is defined through the following Hamiltonian:

$$H = -\sum_{i,j} J_{ij} \vec{s_i} \cdot \vec{s_j}$$

with

$$J_{ij} = \begin{cases} J & \text{if } i,j \text{ are neighbors} \\ 0 & \text{else.} \end{cases}$$

a coupling between spins.

Chapter 5

Implementation

In this thesis Metropolis algorithm was used throughout the calculation. The algorithm applied is of the form of Algorithm (1).

Two series of Monte Carlo simulations were performed :

Non-equilibrium (Varying T)

In this type of experiments we performed a single-flip Metropolis Monte Carlo simulation with varying temperature. Specifically, we choose a temperature range between $T_{initial} = 1$ and $T_{final} = 0.0001$ with a cooling rate equal to the number of iterations. The purpose in this case was to approach the minimum energy of the system as the temperature was gradually lowered down to zero during the MC update to reach the correct ground state. An approach to the correct ground state for a given parameter set was typically reached well within the first 10^7 MC steps.

Equilibrium (Constant T)

In this case we performed a single-flip Metropolis Monte Carlo at fixed temperatures in order to study the effect of temperature in our model. After 10^7 MC iterations at varying temperature, 10^6 more MC steps were imposed at each fixed temperature in order to predict the average configuration of each magnetization component for a given parameter set at a random initial configuration.

Monte Carlo Move

In contrast with the original Ising model (4.2.1) where the spin variable S_i has only two states (up and down),the model we constructed introduces a generalized variable S_i that can take values out of a continuum set of possible states. Specifically,each classical spin $\vec{S_i}$ is taken to have the unit length, $(\vec{S_i})^2 = 1$. Through the simulation, in each transition only one change of the spin sites is occurred on the system until the system approaches the ground state.

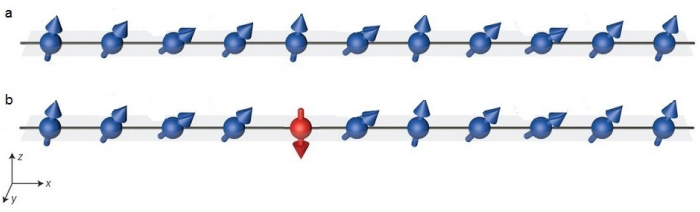

Figure 5.1: A single spin flip in a 1D spin chain where S_i can take values out of a continuum set of possible states.

The new configuration for the spin is proposed by evaluating two random numbers $\phi \in [0, 2\pi]$ and $c = \cos\theta \in [-1, 1]$ and assigning the updated position

$$S(\phi, c) = (\sqrt{1-c^2}\cos\phi, \sqrt{1-c^2}\sin\phi, c)$$

to the chosen spin.

Parameters

In this work $\lambda = 1$ is set in all calculations. Free boundary conditions were imposed on a finite $1 \times N$ chain lattice so that $\vec{S}_1 = \vec{S}_N = 0$. Magnetic field and anisotropy orientation were fixed along the z-direction. Exchange energy term was modified so that zero is the minimum energy of the system. Particularly, in each MC iteration 1 was subtracted from the exchange term.

Lattice Hamiltonian

The following lattice Hamiltonian is regarded as a lattice adaptation of the continuum Hamiltonian (2.6) for the one dimensional case [10],[11]

$$H_{1D} = -J\sum_r \vec{S}_r \cdot \vec{S}_{r+\hat{x}} - DM\sum_r (\vec{S}_r \times \vec{S}_{r+\hat{x}}) \cdot \hat{x} - K\sum_r \vec{S}_{rz}^2 - \vec{H}\sum_r \vec{S}_{rz}$$

Once again, in the discrete problem J is the ferromagnetic exchange constant,DM is the Dzyaloshinskii-Moriya interaction constant, K is the easy-axis anistotropy constant and H is the external magnetic field constant where $\vec{H} = (0, 0, H)$. Magnetic spins are expressed as S_r,where r refers to the position of the spins on a chain lattice.

Usually, the ferromagnetic exchange is the dominant energy scale and corrections to this Hamiltonian are just anisotropies which favor either a certain plane or direction for the magnetization.

5.1 Identification between the lattice and continuum model

Spin interactions can be modeled by the previous one-dimensional (1D) lattice Hamiltonian, once appropriate identification between the lattice and continuum model parameters is made.

Suppose that Δx is the distance between neighboring spins. Then for each term of the energy functional (2.8) we have following transformation :

Exchange energy

Discretizing the term

$$(\partial_x \vec{m})^2 = \frac{1}{\Delta x^2}(\vec{m}_{i+1} - \vec{m}_i)^2 = \frac{1}{\Delta x^2}(\vec{m}_{i+1}^2 + \vec{m}_i^2 - 2\vec{m}_{i+1}\vec{m}_i) = \frac{1}{\Delta x^2}(2 - 2\vec{m}_{i+1}\vec{m}_i)$$

the exchange term becomes

$$\frac{1}{2}\int \partial_x \vec{m} \cdot \partial_x \vec{m} dx \approx \frac{1}{2}\sum_i \frac{-2(\vec{m}_{i+1}\vec{m}_i)}{\Delta x^2}\Delta x = -\frac{1}{\Delta x}\sum_i \vec{m}_{i+1}\vec{m}_i$$

Thus the exchange constant is of the form

$$J = -\frac{1}{\Delta x} \tag{5.1}$$

Dzyaloshinskii-Moriya

For the DM term we have the discretization

$$\vec{m}(\nabla \times \vec{m}) = -\frac{1}{\Delta x}(\vec{m}_i \times \vec{m}_{i+1})\hat{x}$$

Therefore,

$$\lambda \int \vec{m}(\nabla \times \vec{m})dx \approx -\frac{\lambda}{\Delta x}\Delta x \sum_i (\vec{m}_i \times \vec{m}_{i+1})\hat{x}$$

and thus the constant for DM term in the lattice model is

$$DM = -\lambda \tag{5.2}$$

Anisotropy

Similarly for the easy-axis anisotropy term

$$\frac{k_3}{2}\int (1 - m_3^2) \;\; dx \approx \frac{k_3}{2}\sum_i (1 - (m_3^i)^2)\Delta x = \frac{k_3 \Delta x}{2}\sum_i (1 - (m_3^i)^2)$$

and so the lattice anisotropy constant is

$$K = \frac{k_3}{2}\Delta x \tag{5.3}$$

External Field

Finally, for the external field term

$$h_{ext}\int (1 - m_3)dx \approx h_{ext}\sum_i (1 - m_3^i)\Delta x = h_{ext}\Delta x \sum_i (1 - m_3^i)$$

which leads to the identification

$$H = h_{ext} \cdot \Delta x \tag{5.4}$$

Chapter 6

Results

In this Chapter we will examine three different systems, (6.1) Domain Wall, (6.2)Dzyaloshinskii-Moriya interaction and Anisotropy and (6.3)Spiral in the presence of External field. In each case both Non-equilibrium and equilibrium states will be studied.

6.1 Easy-axis Anisotropy : Domain Wall

In the presence of easy axis anisotropy the system is of the form (3.6) and the corresponding magnetization shown in Fig.(3.2) is described from the Eq.(3.11).

According to this expression the minimum energy at $T = 0$ is of the form (3.10).

The parameters used for this simulation are

$$\Delta x = 0.5, k_3 = 1, \lambda = 0 \quad and \quad h = 0$$

For the first series of Monte Carlo simulations we may note the following.

Non-equilibrium (Varying T)

We have performed a simulation with unitless temperature slowly lowered down from 1 to 0.0001. Results of the final state of the system are given in Table(6.1). The information given about this case is that the energy at the end of the simulation reaches the value 2.8935. As we have seen, in this case the corresponding energy is of the form (3.10) and thus for $k_3 = 1$ the minimum energy of a domain wall is 2. We may say that the system has not reach yet a minimum energy state. One reason about that may arise from the fact that m_z is not completely suppressed. At very low T, Monte Carlo algorithm may not yield accurate results, perhaps due to low acceptance probability.

In Fig.(6.1.b,c,d) the evolution of the system at three different temperatures is described. It is clear that as temperature lowers down to zero the system slowly approaches the state with the minimum energy.

As we can see in Fig.(6.1.b,c,d), as temperatures lower down to zero the configuration of the system represents a domain wall solution. Particularly, in the second graph (6.1.b) where T=0.6 the configuration is quite random yet. This is due to the fact that at this state the temperature is quite high and thus spins may take all possible states. Moreover, the number of MC iterations is not large enough at that point and therefore the algorithm has not perform as much spin-flips needed to reach a minimum energy state. On the other hand, in Fig.(6.1.c) for T=0.1, we are able to see that a domain wall solution that goes from $m_z = -1$ to $m_z = 1$ is nearly represented. That becomes clear in Fig.(6.1.d) where for T=0.0001 the spins perform a domain wall solution that goes from $m_z = -1$ to $m_z = 1$.

MC steps	MC move Acceptance (%)	Final Energy
10^7	31.47	2.8935

Table 6.1: Details of non-equilibrium (Varying T) MC simulation of the easy-axis anisotropy system for $\Delta x = 0.5$, $k_3 = 1$, $\lambda = 0$, h=0.

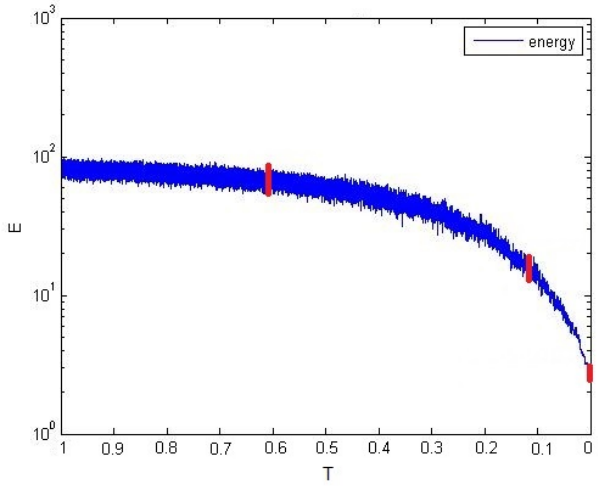

(a) Energy at each MC step

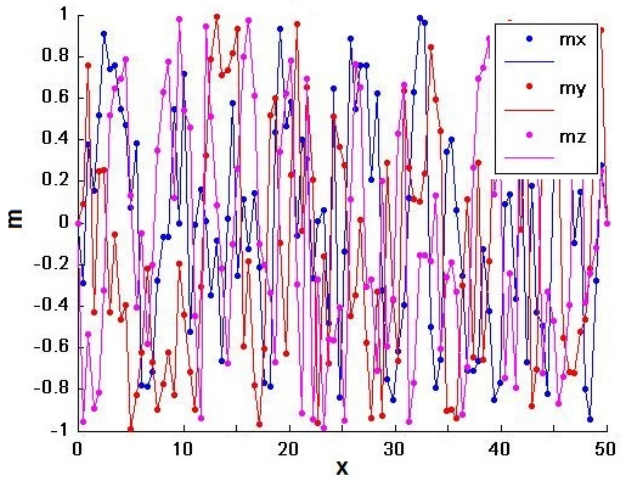

(b)

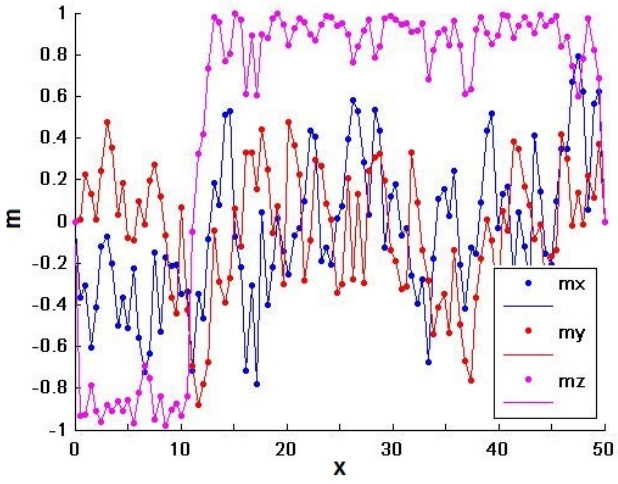

(c)

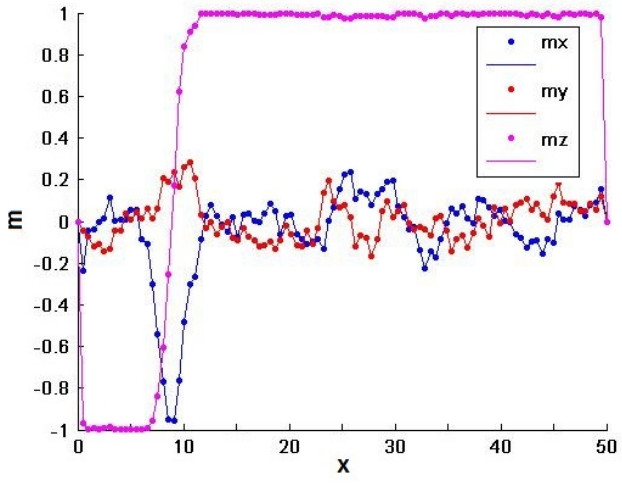

(d)

Figure 6.1: (a)Energy as a function of MC steps for easy-axis anisotropy in non-equilibrium . (b),(c),(d) Snapshots of the evolution of the system at T = 0.6,T=0.1 and T=0.0001 accordingly for $\Delta x = 0.5$, $k_3 = 1$, $\lambda = 0$, h=0.

Equilibrium (Fixed T)

In the second type of Monte Carlo simulations we explored the thermal equilibrium at three different temperatures. In Table(6.2)) are given the detail of each simulation

In Fig.(6.2.a,b,c) we see the average configuration of each component of the spins at specific temperatures.

At high temperature ,T = 0.5, as we can see in Fig.(6.2.a) the mean value of each coordinate of the spins is nearly equal to zero. This is due to the fact that the system is in random configuration and thus it is able to reach all possible states.

As temperature decreases,T =0.1, Fig.(6.2.b) shows that the coordination of the spin in the z-direction tends to approach the -1 value, or in other words the left domain in Fig.(3.2).

For the last graph in Fig(6.2.c) where T= 0.001, the system is trapped in a configuration since the temperature is not close enough to T =0.

Furthermore, from the information provided from Table(6.2) we see that at high temperatures the acceptance of the Monte Carlo move as well as the energy of the system is greater. This is due to the fact that in high temperatures spins may take all possible values and hence the entropy of the system is greater. At this point we may recall that the configuration probability is given by the Boltzmann distribution with inverse temperature $\beta \geq 0$, described in Eq.(4.1.2), tells us that in high temperatures the probability is higher.

At T=0.001 the MC acceptance rate is too low as it possibly needed another MC step updating algorithm or otherwise more MC steps for the same error.

Moreover it is clear that for lower temperatures the standard deviation (σ) is larger since there are more statistical independent samples.

At this moment we should note that those results may depend on the rate of cooling in analogy to simulated annealing.

Results				
	Temperature	MC move Acceptance(%)	Mean Energy	Standard Deviation(σ)
Fig. 6.2.a	0.5	33.30	60.0289	4.0922
Fig. 6.2.b	0.1	4.78	12.9009	3.5078
Fig. 6.2.c	0.001	0.14	5.4819	4.6489

Table 6.2: Details of equilibrium (fixed T) MC simulations of easy-axis anisotropy system for $\Delta x = 0.5$, $k_3 = 1$, $\lambda = 0$, h=0.

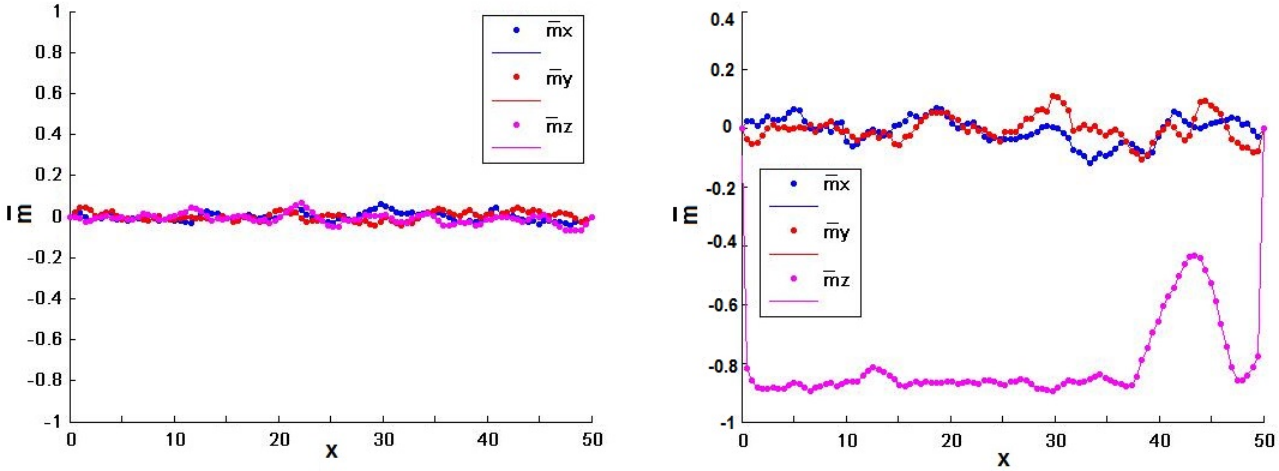

(a) (b)

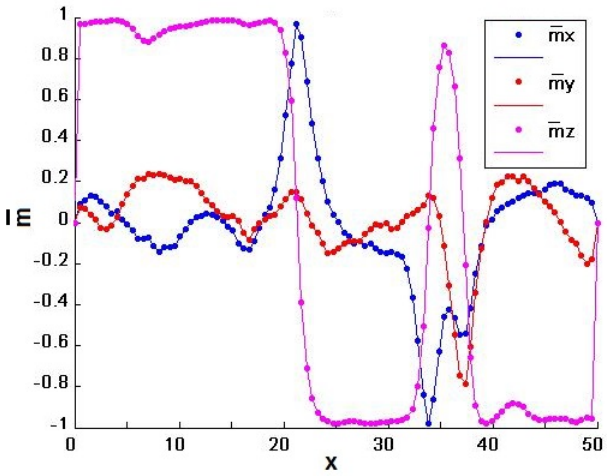

(c)

Figure 6.2: Average configuration of each spin component for the easy-axis anisotropy system at (a)T=0.5,(b)T=0.1,(c)T=0.01, for $\Delta x = 0.5$, $k_3 = 1$, $\lambda = 0$, h=0.

6.2 Dzyaloshinskii-Moriya interaction and Anisotropy

In this section we will investigate a system with Dzyaloshinskii-Moriya interaction and Anisotropy. We examine the cases

i) Zero anisotropy constant

ii) Anisotropy constant below k_c

iii) Anisotropy constant near k_c

iv) Anisotropy constant above k_c

where k_c is the critical value for anisotropy and is of the form (3.15).

6.2.1 Zero Anisotropy constant ($k_3 = 0$)

In the absence of anisotropy the solution of the system is of the form (3.12) and it is called spiral. The graph of the magnetization for $\lambda = 1$ is shown in Fig.(3.3). The period of the spiral solution here is 2π. The average energy density over a period L is of the form (3.13).

In this case we will use for the simulation the parameters

$$\Delta x = 0.5, k_3 = 0, \lambda = 1, h = 0$$

For the first series of Monte Carlo simulations we may note the following.

Non-equilibrium (Varying T)

In this type of simulation we examine the behavior of the system as temperatures lower nearly down to zero for a spiral system.

As we have seen, in a system with DM interaction is possible for energy to take negative values since the Dzyaloshinskii-Moriya term is able to take both positive and negative values. Of what is know, the energy of a spiral solution can reduced below the energy of the ferromagnetic state where the minimum energy is zero, as a domain wall is inserted in the system. In this case, after 10^7 MC steps, as we can see in Table(6.3) the final energy is -9.4556.

Next, we calculate the average energy density over a period L that is of the form (3.13). The average energy density over a period 2π for $\lambda = 1$ is -0.5. Hence, to find out how many times the domain wall will be repeated we calculate $50/2\pi \approx 8$. In Fig.(6.3.d) we see that we have about 7 repeated domain walls with period 2π in the space $(0, 50)$.

Now we are able to calculate the minimum energy of the spiral solution which is $-0.5 \times 8 = -4$ since there are only 8 periods and the energy per period is -0.5. It is clear the the final energy found for this system that is -9.4556 is quite far from the minimum energy of the solution at T = 0. One possible reason about this is that the size of the box of the simulation is not an integer multiple of the period. Moreover, the free boundary conditions at the edges of the chain lattice do not allow the spins at the edge to move freely.

More details about the spiral configuration are given in Fig.(6.3.b,c,d) where the evolution of the system through the simulation as the temperatures lowers down is presented. Specifically, we are able to see the snapshots of the system at three different temperatures.

In Fig.(6.3.b) for T=0.6, the system has a random configuration. As the temperature lowers to T=0.1, in Fig.(6.3.c), it is certain that the systems is spiral with a period around 2π. In the final state of the configuration in Fig.(6.3.d), after 10^7 MC iterations at T = 0.0001 ,it is clear that the system slowly approaches a spiral solution with period 2π.

MC steps	MC move Acceptance(%)	Final Energy
10^7	29.49	-9.7095

Table 6.3: Details of non-equilibrium (Varying T) MC simulation of the zero anisotropy system for $\Delta x = 0.5$, $k_3 = 0$, $\lambda = 1$, h=0.

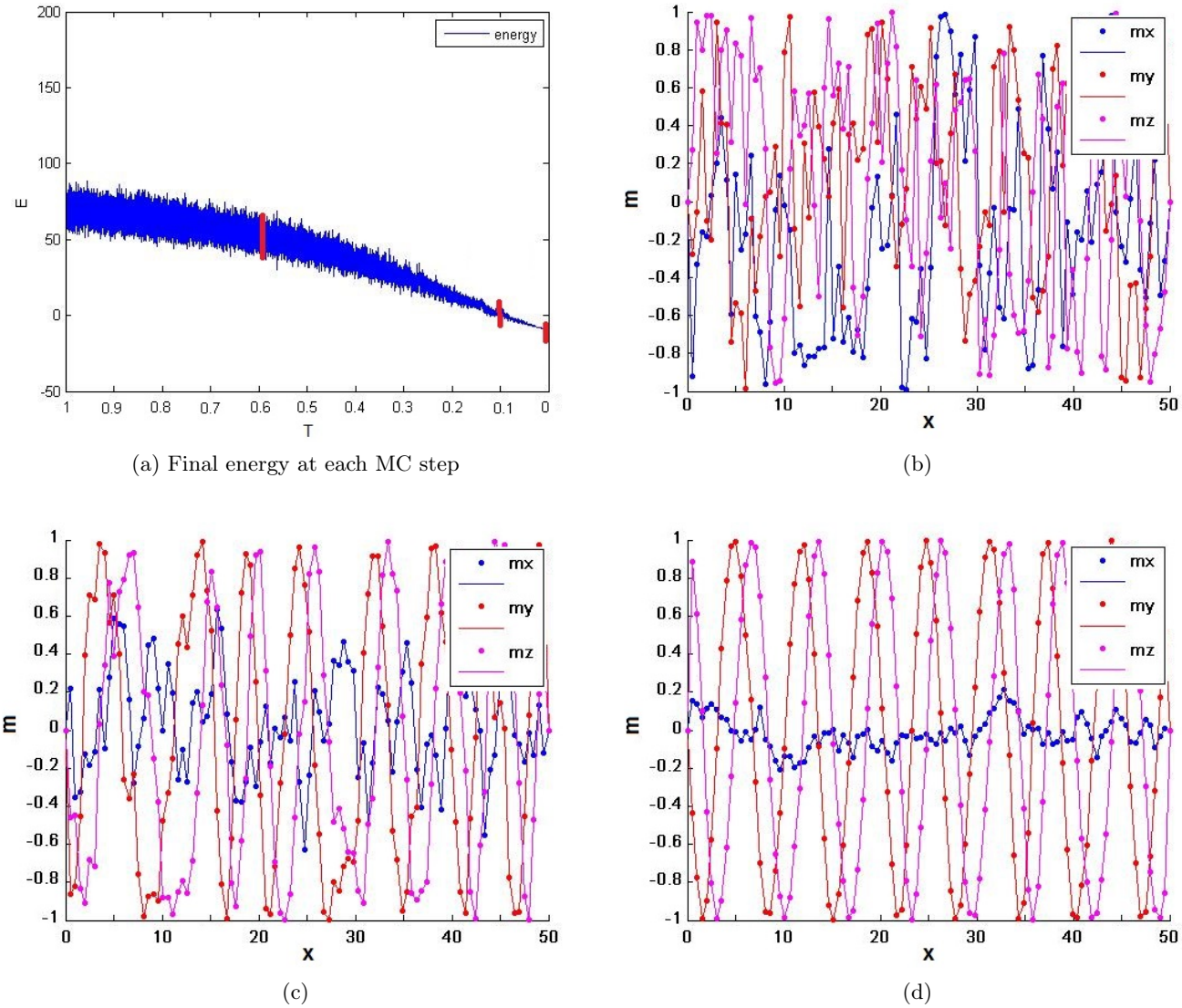

(a) Final energy at each MC step

(b)

(c)

(d)

Figure 6.3: (a)Energy as a function of MC steps for zero anisotropy in non-equilibrium. (b),(c),(d) Snapshots of the evolution of the system at T=0.6,T=0.1 and T=0.0001 accordingly for $\Delta x = 0.5$, $k_3 = 0$, $\lambda = 1$, h=0.

Equilibrium (Fixed T)

In this case we perform a simulation at three different temperatures.

In Fig.(6.4.a,b,c) the graph the mean value of the components of each spin is given. What is clear, is that as the energy lowers down to zero we have a spiral solution.

As we can see in Fig.(6.3.a) for a high temperature, T=0.5, the mean configuration of the components of the spins is nearly zero. This is a result of the fact that entropy of the systems is high and the spins may take all possible values. Accordingly, the energy of the system is greater. The acceptance of the Monte Carlo move is also bigger for high temperatures since of the Boltzmann distribution (4.1.2).

In in Fig.(6.3.b) as temperature lowers,T=0.1, the configuration of the system tends to perform a graph of a spiral solution. Subsequently, in Fig.(6.3.c) as the temperature lowers down even more to zero specifically to T=0.001, one may observe that the system slowly reaches the spiral configuration at T=0.

Note that in this case the highest temperature corresponds to a thermal energy that is comparable to the energy density (-0.5) of the spiral solution.

Moreover it is clear that for lower temperatures the standard deviation (σ) is larger since there are more statistical independent samples.

Results				
	Temperature	Acceptance of MC move (%)	Mean Energy	Standard Deviation (σ)
Fig. 6.4.a	0.5	30.72	36.6059	4.4689
Fig. 6.4.b	0.1	4.79	0.8036	3.6313
Fig. 6.4.c	0.001	0.16	-5.9086	4.8890

Table 6.4: Details of equilibrium (fixed T) MC simulations of zero anisotropy system for $\Delta x = 0.5$, $k_3 = 0$, $\lambda = 1$, h=0.

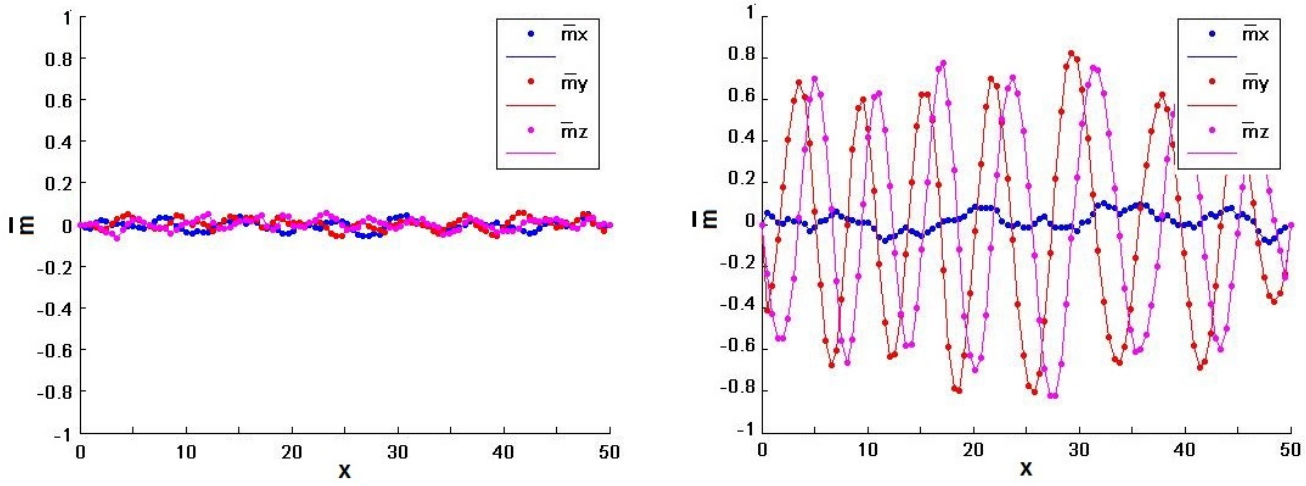

(a) (b)

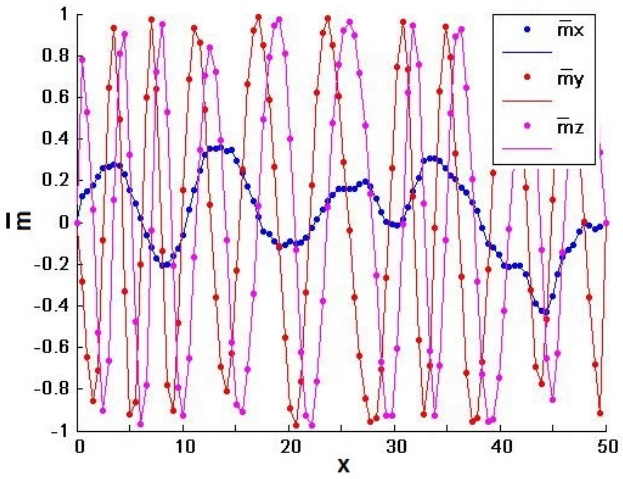

(c)

Figure 6.4: Average configuration of each spin component for zero anisotropy at (a)T=0.5,(b)T=0.1,(c)T=0.01, for $\Delta x = 0.5$, $k_3 = 0$, $\lambda = 1$, h=0.

In the following paragraphs we will examine the behavior of the system for an anisotropy constant below the critical anisotropy value.

6.2.2 Anisotropy constant below k_c ($k_3 < k_c$)

As we have seen in Eq.(3.15) the critical point is equal to $k_c = \frac{\pi^2}{4}\lambda^2$. Hence for $\lambda = 1$ $k_c = \frac{\pi^2}{4} \approx 2.46$.

For an anisotropy constant below the critical value the energy is negative as we have shown in Eq.(3.15). That leads as to conclusion that the configuration of the system will be spiral. As we have seen spiral solution is of the form (3.12) and the spin configuration can be represented as in Fig. (3.3). Moreover, the average energy density is -0.5. Since the spiral solution consists of a proliferation of domain walls the energy density of the system will be above -0.5 and below 0.

In this case we will use for the simulation the parameters

$$\Delta x = 0.5, k_3 = 1, \lambda = 1, h = 0$$

Non-equilibrium (Varying T)

In this case after performing 10^7 MC steps the minimum energy of the system is -4.0125. It is clear then that the energy of the system is reduced below the energy of the ferromagnetic state. Therefore, we may expect that the solution of this system will be spiral.

In Fig.(6.5.a,b,c) we may see the evolution of the system as the temperatures lowers down to zero. In particular, in Fig.(6.5.b) one can see that the system has a random configuration due to the high temperature T=0.6 as well as the small number of Monte Carlo iterations.

On the other hand, in Fig.(6.5.c,d) it becomes clear that the system is spiral. At this state it is obvious that there is indeed a periodic proliferation of domain walls. Each domain wall is repeated after a nearly 2π period.

Hence, the average energy density of the spiral solution is indeed -0.5. The number of domain walls inserted to the system should be $50/2\pi \approx 8$ in the space $(0, 50)$. However, as we can see in Fig.(6.5.d) the number of domain walls inserted to the system is nearly 6. One possible reason about this is that the size of the box of the simulation is not an integer multiple of the period. The energy density in this case is $-4.0125/50 \approx -0.08$. The final energy of the system after the simulation is -3.6891 that is close to -4 as expected in theory.

It is important to note here that in this case where we have add the anisotropy term to the system we observe that anisotropy affects the length of the period.

Some significant difference with the case of $k_3 = 0$ is that in this case the presence of DMI term leads the system to spiral solution at T=0 at higher temperatures. Moreover, the energy in this case is much more closer to the theoretical approach.

MC steps	MC move Acceptance (%)	Final Energy
10^7	29.29	-3.6891

Table 6.5: Details of non-equilibrium (Varying T) MC simulation where anisotropy is below critical anisotropy point for $\Delta x = 0.5$,$k_3 = 1$, $\lambda = 1$, h=0.

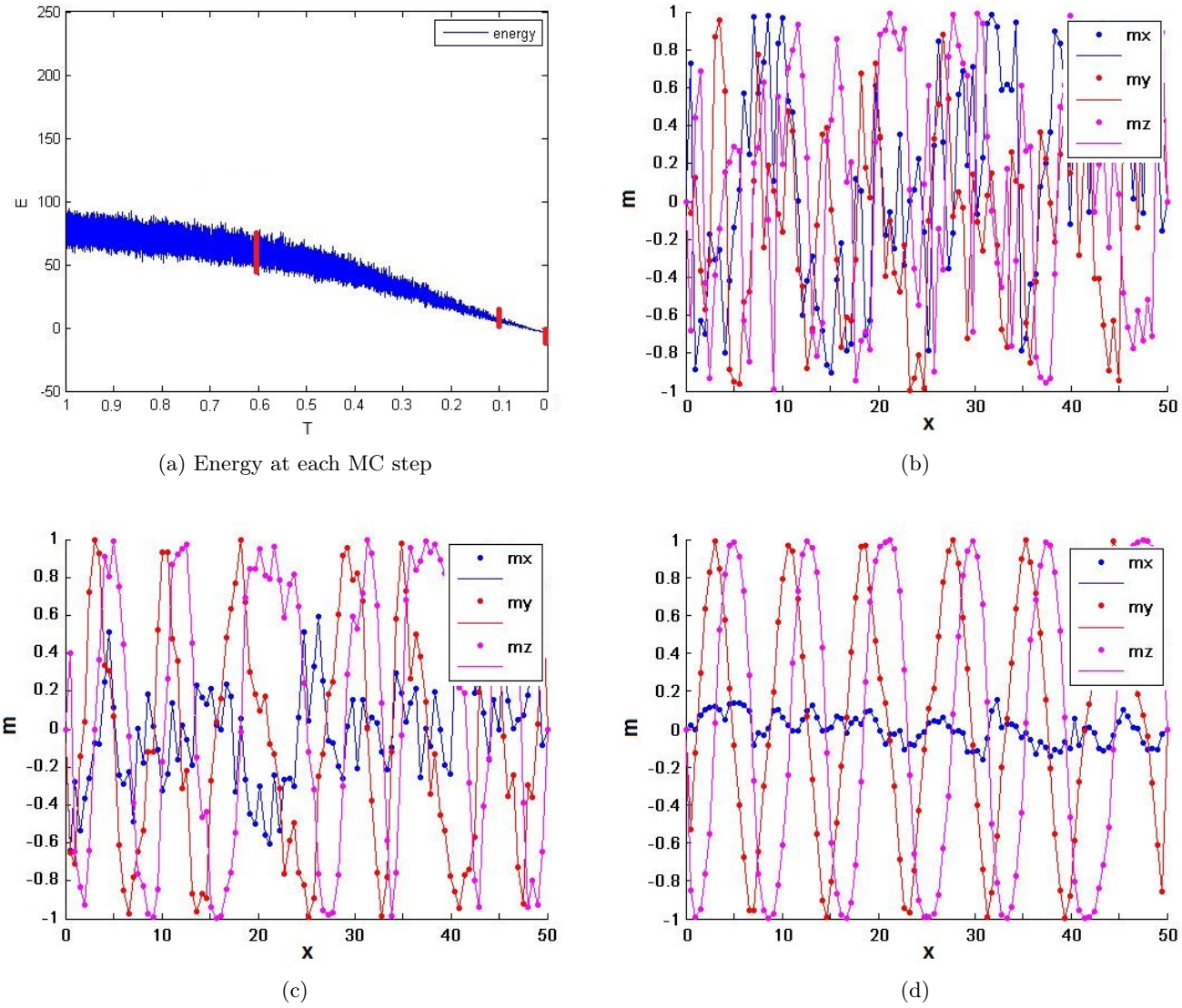

(a) Energy at each MC step

(b)

(c)

(d)

Figure 6.5: (a)Energy as a function of MC steps for anisotropy below critical anisotropy point in non-equilibrium. (b),(c),(d) Snapshots of the evolution of the system at T = 0.6,T=0.1 and T=0.0001 accordingly for $\Delta x = 0.5$,$k_3 = 1$, $\lambda = 1$, h=0.

Equilibrium (Fixed Temperature)

In this section we will study the effect of the temperature on our system.

The average configuration of the components of spins after an impose of 10^6 MC iterations to the system for fixed temperatures is given in Fig.(6.6.a,b,c).

What is clear in Fig.(6.6.a) is that for a high temperature,T=0.5, spins move around zero. The reason is the configuration is random and spins are able to take all possible values. Thus the mean value of the energy is also higher. Furthermore due to the Boltzmann probability calculation it is clear that the acceptance of the Monte Carlo move will be higher too, what is true if we consider the results give in Table(6.6).

As we reach lower temperatures ,T=0.1, as in Fig.(6.6.b), the system seems to approach a minimum energy state and a spiral configuration at T=0. Moreover for lower temperatures the standard deviation (σ) is larger since there are more statistical independent samples. Particularly, high standard deviation indicates that the data points are spread out over a wider range of values.

In compare with the the system with $k_3 = 0$ we see that in this case the statistical error σ is slightly smaller but it is still large enough.

As we move to Fig.(6.6.c) for T=0.001 the system is almost in a spiral solution form(3.11). The period of the repetition of the domain wall is nearly 2π and the value of the average energy of the system is negative as expected. At this temperature we may observe that the mean value of the energy is negative as we expected for the spiral case.

Results				
	Temperature	Acceptance of MC move (%)	Mean Energy	Standard Deviation(σ)
Fig. 6.6.a	0.5	30.44	52.1745	4.5176
Fig. 6.6.b	0.1	4.60	6.6625	3.6305
Fig. 6.6.c	0.001	0.13	-2.3114	4.7330

Table 6.6: Details of equilibrium (fixed T) MC simulations where the anisotropy is below critical anisotropy point for $\Delta x = 0.5$,$k_3 = 1$, $\lambda = 1$, h=0.

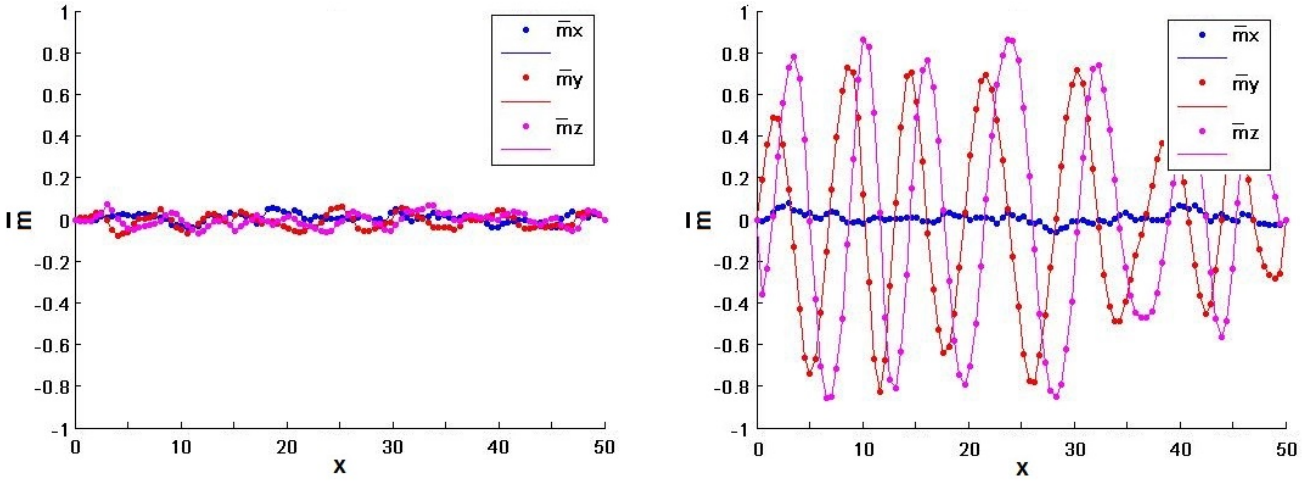

(a) (b)

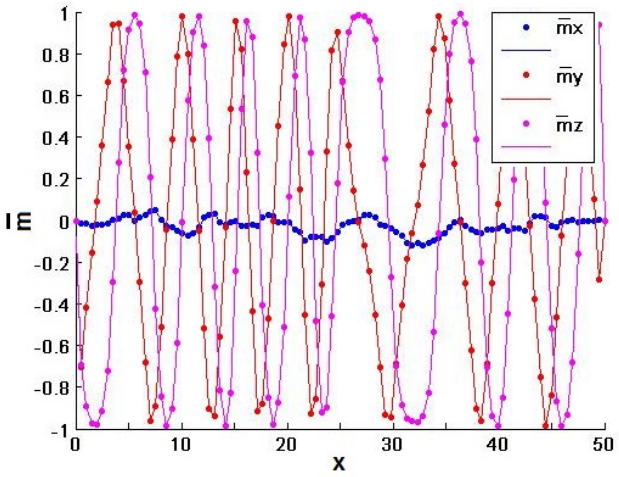

(c)

Figure 6.6: Average spin configuration configuration of each spin component for anisotropy below critical anisotropy point at (a)T=0.5,(b)T=0.1,(c)T=0.01,for $\Delta x = 0.5$,$k_3 = 1$, $\lambda = 1$, h=0.

6.2.3 Anisotropy constant above k_c ($k_3 > k_c$)

Increasing the anisotropy constant one possible solution is a domain wall solution where the energy of the domain wall form (3.14). Here we expect the energy to be positive and thus we expect the minimum energy of the system to be equal to $2\sqrt{k_3} + \lambda\pi$.

Another possible solution in this case is the simplest solution of all where spins take the values $(0, 0, \pm 1)$. Else the system will prefer a spiral solution.

In this case we will use for the simulation the parameters

$$\Delta x = 0.5, k_3 = 6, \lambda = 1, h = 0$$

Non-equilibrium (Varying Temperature T)

As we can see in Fig.(6.7.a) and Table(6.7) the final energy of the system is 2.9085. Therefore we are able to assume that the system has a domain wall solution. We should be also aware that the system has not yet reached a minimum energy state since the minimum energy of a domain wall in this case is $2\sqrt{6} - \pi = 1.7573$. One possible reason that the system has not reached yet a minimum energy state is probably because the energy is still high enough and thus the temperature should be further lowered down or the Monte Carlo iterations should be increased.

We may observe in Fig.(6.7.b) that for a high temperature, T=0.6, spins perform a random configuration due to the fact that at high temperatures the entropy of the system is larger.

On the other hand ,in Fig.(6.7.c) where T= 0.1 one may observe that the systems slowly seems to take the form of a domain wall solution going from $m_z = 1$ to $m_z = -1$.

At the final state of the simulation in Fig.(6.7.c) where the temperature is the lowest with T=0.0001, it is finally obvious that the system fa domain wall solution going from $m_z = 1$ to $m_z = -1$.

MC steps	MC move Acceptance (%)	Final Energy
10^7	26.10	2.9085

Table 6.7: Details of non-equilibrium (Varying T) MC simulation of the system where anisotropy is above the critical anisotropy point for $\Delta x = 0.5$,$k_3 = 6$, $\lambda = 1$, h=0.

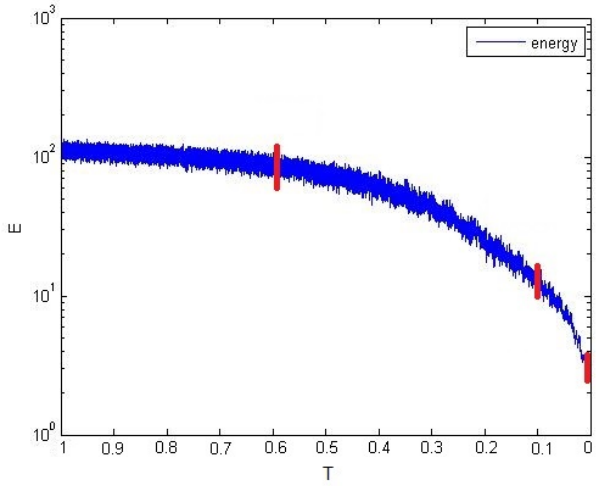

(a) Energy at each MC step

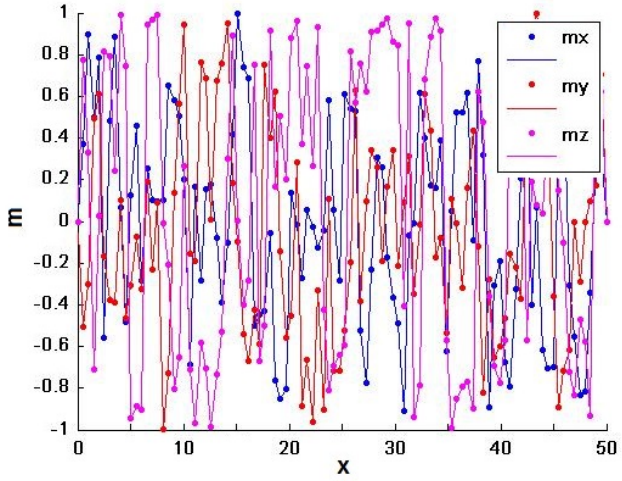

(b)

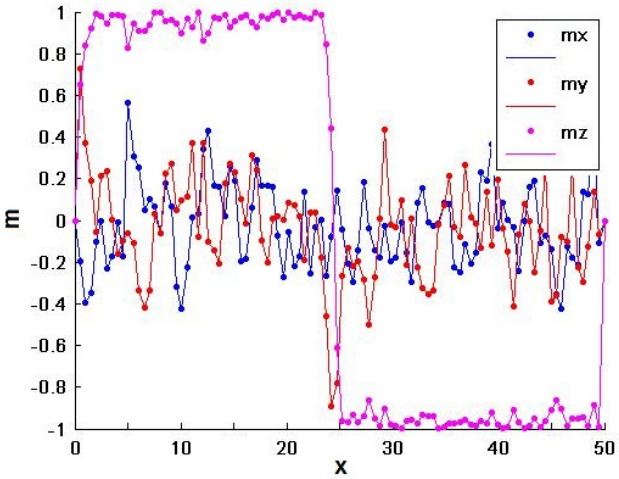

(c)

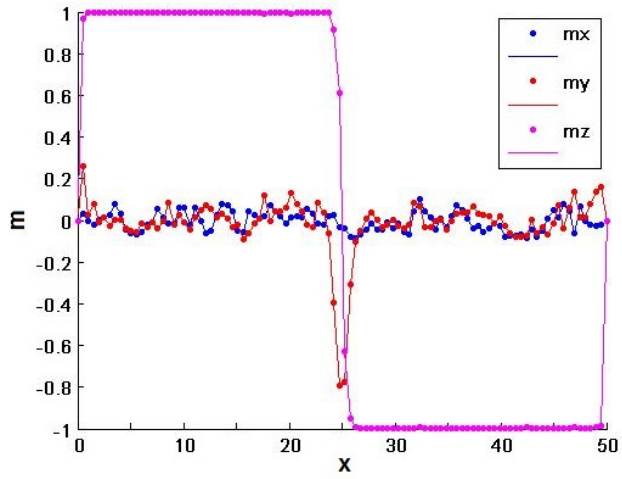

(d)

Figure 6.7: (a)Energy as a function of MC steps for anisotropy above the critical anistotropy point in non-equilibrium. (b),(c),(d) Snapshots of the evolution of the system through MC iterations at T = 0.6, T=0.1 and T=0.0001 accordingly for $\Delta x = 0.5$,$k_3 = 6$, $\lambda = 1$, h=0.

Equilibrium (Fixed Temperature)

Here we examine the effect of temperature to the system after a simulation of 10^6 Monte Carlo iterations for specific values of temperature.

The mean configuration of the spin components at certain values of temperature is given in Fig.(6.8.a,b,c). One can see that the more the temperature decreases to zero, the more the system tends to a better equilibrium state.

In Fig.(6.8.a) it is clear that for a high temperature,T=0.5, spins move around zero. The reason is the configuration is random and spins are able to take all possible values. Thus the mean value of the energy is also higher. Furthermore due to the Boltzmann probability calculation it is clear that the acceptance of the Monte Carlo move will be higher too, what is true based on the results give in Table(6.8).

On the other hand, in Fig.(6.8.b) where the temperature is further lowered to T=0.1, one can estimate that the system will behave as a spiral solution at the beginning.

At the lowest temperature T=0.001, it is clear in Fig.(6.8.c), that at the beginning of the simulation spins in z-direction favor both orientations ± 1. Thus there are two degenerate ground states for the system where $m = \pm(0, 0, 1)$. What is interesting in this figure is that as the simulation continues one can see that the spins seem to try to reach a spiral solution.

We may claim then that the configuration of the average spin components is a combination of a uniform solution where $m = \pm(0, 0, 1)$ and a spiral solution. From another aspect, one may claim that the system is spiral where its period is suddenly reduced. The reason of this behavior is that the MC acceptance rate is too low as it possibly needed another MC step updating algorithm or otherwise more MC steps for the same error.

As shown in Table(6.8) standard deviation increases as temperature lowers. High standard deviation indicates that the data points are spread out over a wider range of values.

Results				
	Temperature	Acceptance of MC move (%)	Mean Energy	Standard Variation(σ)
Fig. 6.10.a	0.5	26.06	75.1762	5.9711
Fig. 6.10.b	0.1	3.68	22.5076	5.3979
Fig. 6.10.c	0.001	0.12	12.2890	6.7785

Table 6.8: Details of equilibrium (fixed T) MC simulations of the system where anisotropy is above the critical anisotropy point for $\Delta x = 0.5$,$k_3 = \pi$, $\lambda = 1$, h=0.

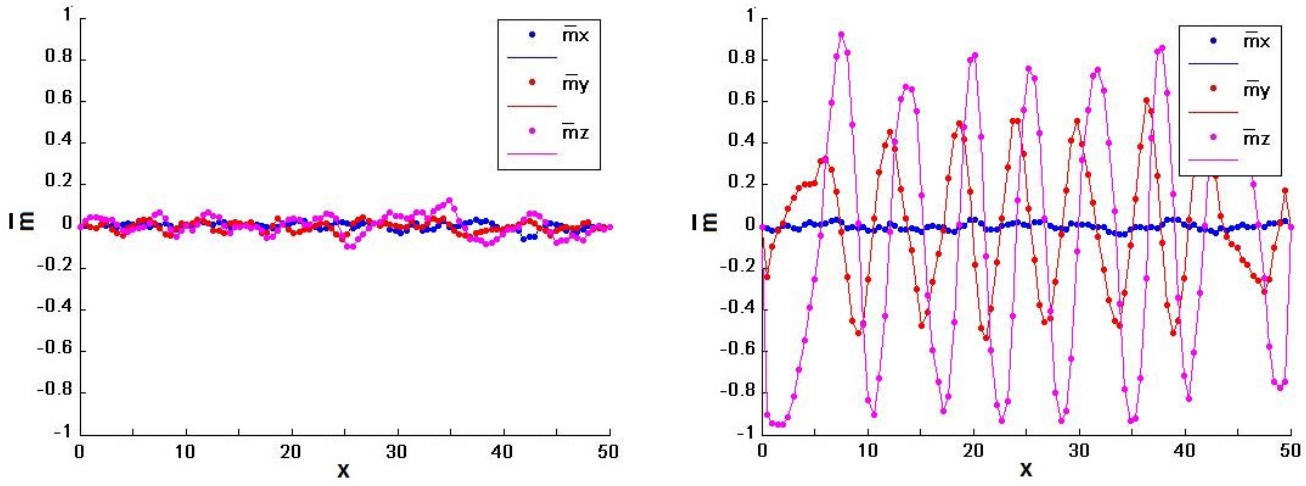

(a) (b)

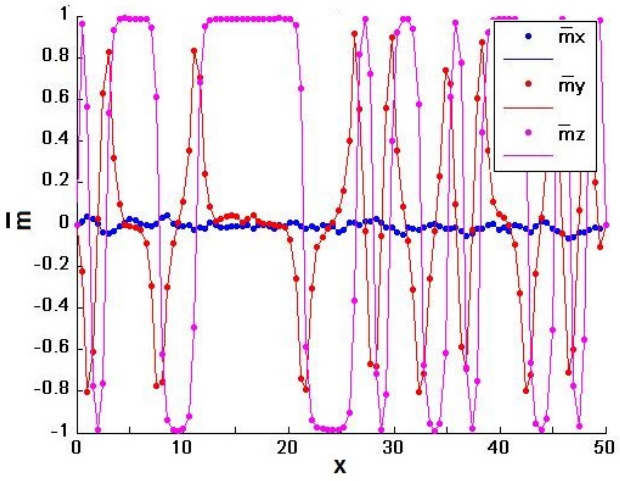

(c)

Figure 6.8: Average configuration of each spin component where anisotropy is above the critical anisotropy point at (a)T=0.5,(b)T=0.1,(c)T=0.01, for $\Delta x = 0.5$,$k_3 = 6$, $\lambda = 1$, h=0.

6.3 Spiral in the presence of External field

In this section we will investigate a spiral system in the presence of external field for the cases

i) External field constant above h_c

ii) External field constant below h_c

where h_c is the critical value of the external field for the system. The critical external point for this system if of the form (3.20).

In the following paragraphs we will examine the behavior of the system for an external field constant below the critical external field value.

6.3.1 External field constant below h_c ($h < h_c$)

In the total absence of easy-axis anisotropy the system is of the form (3.16) and its solution is given implicitly from Eq.(3.17), a periodic function with period (3.18). The optimized average energy density is given from the Eq.(3.19).

The parameters used for this simulation are

$$\Delta x = 0.5, k_3 = 0, \lambda = 1 \quad and \quad h = 0.5$$

Hence for $\lambda = 1$ the external field interaction constant is $h_c = \frac{\pi^2}{16} \approx 0.61$.

In the following paragraphs we will examine the behavior of the system for an external field constant below the critical external field value.

Non-equilibrium (Varying T)

In this section we study the approach of minimum energy of the system at T=0. In Table(6.9) the information given about the final state of the system show that the energy of system is 1.6782.

At a large temperature T = 0.6 ,the system in Fig.(6.9.b) has a random configuration since the system has not performed enough Monte Carlo iterations and its entropy is large enough. Although as the temperature is lowered to T=0.1, in Fig.(6.9.c) we can see that $m_z = 1$ is favored at some points but the system seems to approach a spiral configuration. In Fig.(6.9.d) at the final state, after 10^7 MC iterations , for T=0.0001 it is clear that there is a proliferation of domain walls.

Since the system is spiral the average energy density is -0.5. Hence we expect the minimum energy density to be above -0.5 and below zero. Here, the minimum energy density is $1.6782/50 \approx 0.008$ which satisfies the previous condition. Though it is clear that the system is far from the minimum energy state. One possible reason is that the MC iterations are not enough and temperature should be further lowered down.

Here we are not able to calculate the number of domain walls appearing in the configuration since the approach has not reached well yet to lowest energy state as period of the domain walls is not constant.

MC steps	MC move Acceptance (%)	Final Energy
10^7	29.20	0.4179

Table 6.9: Details of non-equilibrium (Varying T) MC simulation of the system where external field is below the external field critical point for $\Delta x = 0.5$,$k_3 = 0$, $\lambda = 1$, h=0.5.

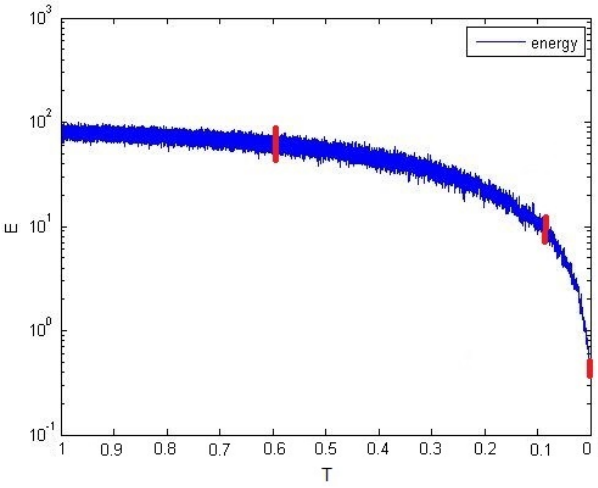

(a) Final energy at each MC step

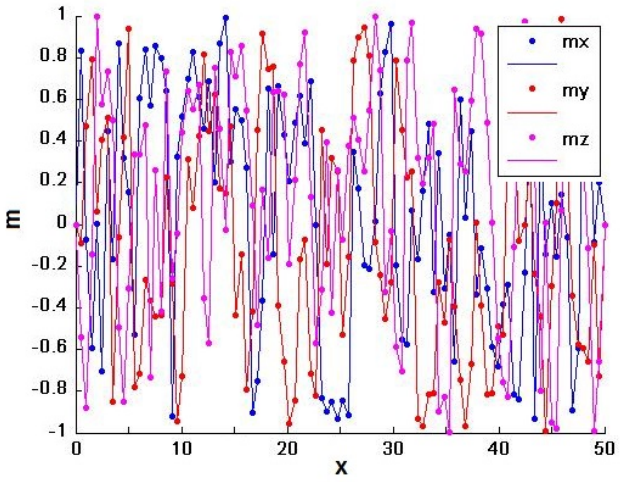

(b)

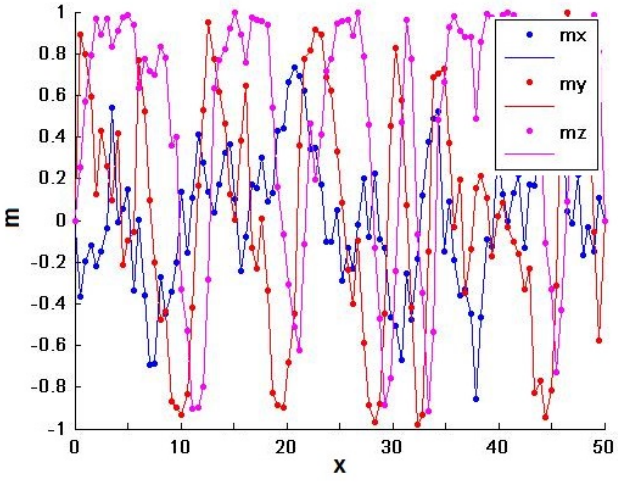

(c)

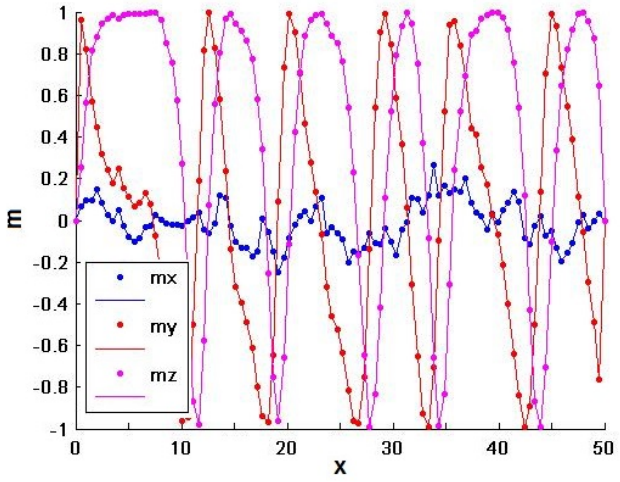

(d)

Figure 6.9: (a)Energy as a function of MC steps for external field below the critical external field point in non-equilibrium. (b),(c),(d) Snapshots of the evolution of the system at T = 0.6,T=0.1 and T=0.0001 accordingly for $\Delta x = 0.5$,$k_3 = 0$, $\lambda = 1$, h=0.5.

Equilibrium (Fixed T)

In this case we study the effect of a fixed temperature applied in our system where the external field is lower than the the external critical point.

At a high temperature T=0.5 , as in Fig.(6.10.a), we can see that the m_x and m_y coordinates of the spins move around zero in contrast with the spins in the z-direction that are reaching slightly higher values because of the external field that favors the values $m_z = 1$.

After that observation one may expect that the spin configuration would perform for lower temperatures a positive domain with $m_z = 1$ favored. Instead, in Fig.(6.10.b) for a lower temperature T=0.1, the spins seem to approach a spiral configuration.

At the lowest temperature T=0.001 , Fig.(6.10.c) shows that the system is indeed spiral but is still far from the configuration of the minimum energy state.

The acceptance of flipping a spin is lowered as the temperature approaches to zero. This is explained after the Boltzmann probability where for lower temperatures the probability is lower. The average energy is strongly connected to the acceptance number of the Monte Carlo move and thus it behaves accordingly.

Moreover it is clear that for lower temperatures the standard deviation (σ) is larger since there are more statistical independent samples.

Results				
	Temperature	Acceptance of MC move (%)	Mean Energy	Standard Variation(σ)
Fig. 6.12.a	0.5	30.26	54.5632	4.7337
Fig. 6.12.b	0.1	4.80	11.0538	3.5937
Fig. 6.12.c	0.001	0.15	2.0923	4.8944

Table 6.10: Details of equilibrium (fixed T) MC simulations for the system where the external field is below the critical external field point, for $\Delta x = 0.5$,$k_3 = 0$, $\lambda = 1$, h=0.5.

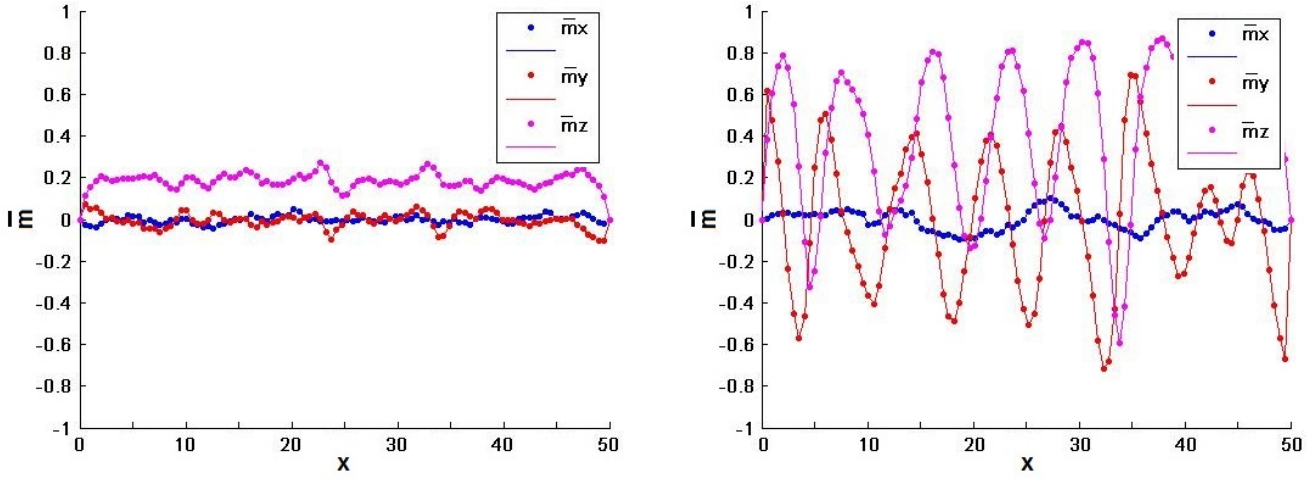

(a)

(b)

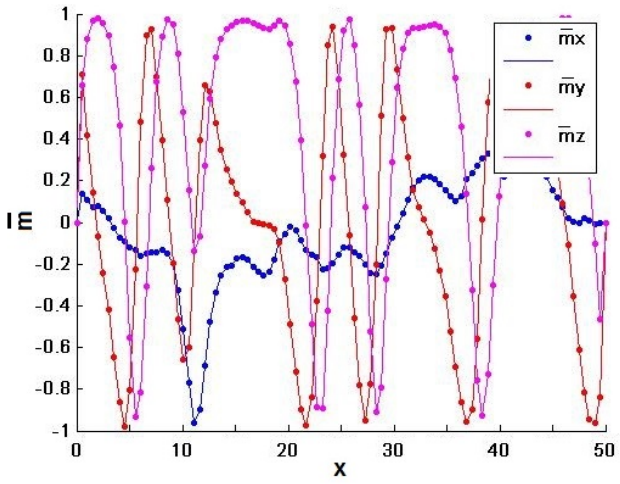

(c)

Figure 6.10: Average spin configuration for external field above the critical external field point at a)T=0.5,(b)T=0.1,(c)T=0.01, for $\Delta x = 0.5$,$k_3 = 0$, $\lambda = 1$, h=0.5.

6.3.2 External Field constant above h_c ($h > h_c$)

By increasing the external field constant the system is again of the form (3.16) and its solution is given implicitly from Eq.(3.17), a periodic function with period (3.18). The optimized average energy density is given from the Eq.(3.19).

The parameters used for this simulation are

$$\Delta x = 0.5, k_3 = 0, \lambda = 1 \quad and \quad h = 1$$

.

Non-equilibrium (Varying T)

In the following paragraphs we will study the non-equilibrium state of the system and its behavior as it approaches the minimum energy state at T=0.

As we can see in Fig.(6.11.a) the energy at the final state of the simulation is 1.6781. The solution we expect should not be for sure a spiral solution. One possible state would be either the uniform state or the domain wall solution.

In Fig.(6.11.b) the configuration is random and inaccurate since at that state for T=0.6 the spin can take all possible values.

As the temperature lowers gradually to to T=0.1, we can see in Fig.(6.11.b) that the spins in the z-direction seem to favor $m_z = 1$ and spins in x,y-directions move around zero. Hence one may expect that the spin configuration as the temperature lowers even more the domain with $m_z = 1$ will be favored. Furthermore, the solution of the system will be $m = (0, 0, 1)$ and the system will be in the ferromagnetic,or equally uniform, state.

As we have expected, in Fig.(6.11.d) spins favor the $m_z = 1$ domain of the domain wall solution shown in Fig.(3.2). The solution of the system is the uniform with magnetization $m = (0, 0, 1)$.

The minimum energy of a uniform solution is zero. Comparing the minimum energy of the uniform solution to the minimum energy of simulation that is 1.6781 we may claim that the system has not reached yet a minimum energy state.

Final Results		
MC steps	MC move Acceptance(%)	Final Energy
10^7	28.39	1.4133

Table 6.11: Details of non-equilibrium (Varying T) MC simulation of the system where external field is above critical external field point for $\Delta x = 0.5$,$k_3 = 0$, $\lambda = 1$, h=1.

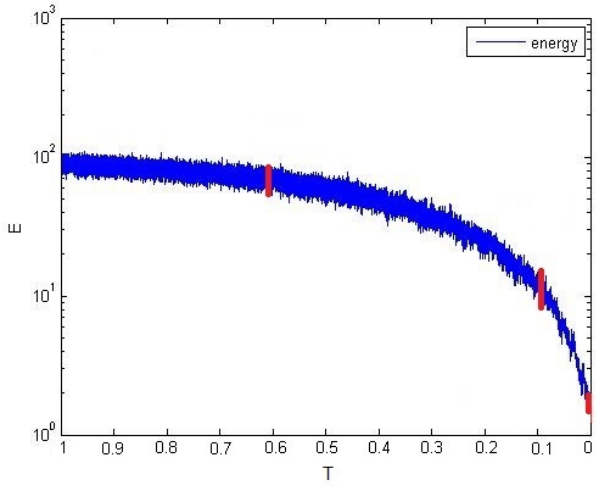

(a) Final energy at each MC step

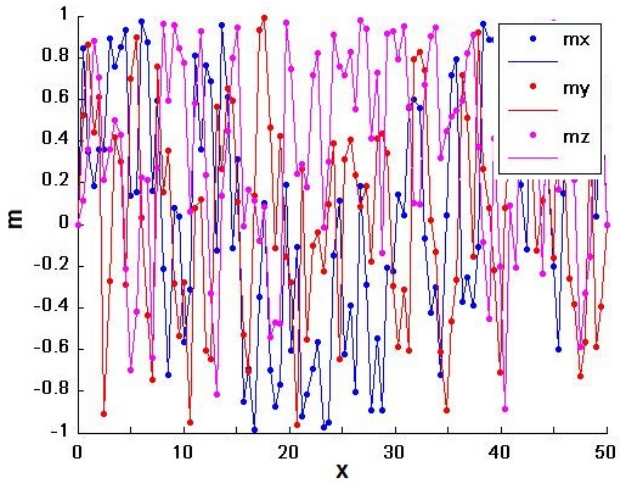

(b)

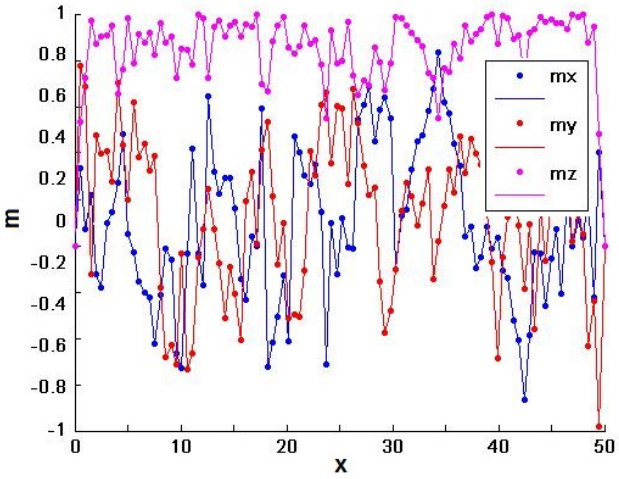

(c)

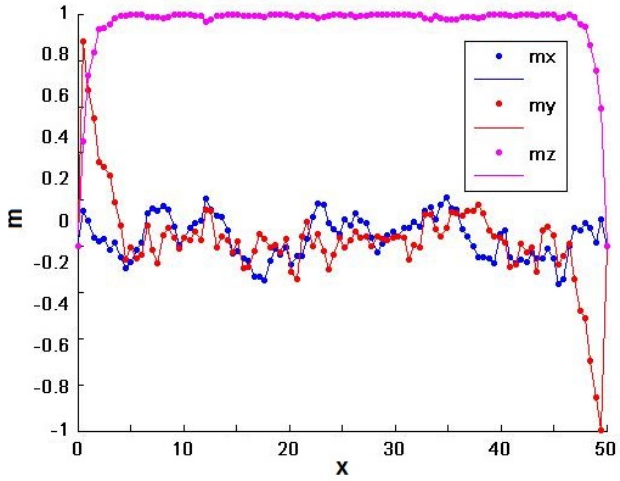

(d)

Figure 6.11: (a)Energy as a function of MC steps for the system where external field is above critical external field point in non-equilibrium . (b),(c),(d) Snapshots of the evolution of the system at T = 0.9,T=0.7 and T=0.0001 accordingly for $\Delta x = 0.5$,$k_3 = 0$, $\lambda = 1$, h=1.

Equilibrium (Fixed T)

In this case we study the effect of a fixed temperature applied in our system where the external field is larger than the the external critical point.

At a high temperature,T=0.5, in Fig.(6.12.b) we can see that the m_x and m_y coordinates of the spins move around zero. On the contrary the spins in z-direction are taking slightly higher values above zero. This is due to the fact that the external field term by its construction favor the $m_z = 1$ values.

Once again one may expect that in this case the spin configuration would perform for lower temperatures a domain with $m_z = 1$ favored or in other words a uniform state with the solution $m = (0, 0, 1)$.

As we have predicted in Fig.(6.12.c) for a lower temperature ,T=0.1, the spin configuration is given by the domain where $m = (0, 0, 1)$ of a domain wall solution as in Fig.(3.2).

At an even lower temperature ,T=0.01, Fig.(6.12.d) shows that the system seems to be spiral with a proliferation of domain walls but for further Monte Carlo iterations we may claim that the system will finally reach the ferromagnetic state where $m = (0, 0, 1)$.

The acceptance of flipping a spin is lowered as the temperature approaches zero temperature. As we have explained in previous cases this is a result of the calculation of the Boltzmann probability given in Eq.(4.1.2). The average energy is strongly connected to the acceptance number of the Monte Carlo move and thus it behaves accordingly.

Moreover it is clear that for lower temperatures the standard deviation is larger since there are more statistical independent samples. As we know high standard deviation indicates that the data points are spread out over a wider range of values.

Results				
	Temperature	Acceptance of MC move (%)	Mean Energy	Standard Variation(σ)
Fig. 6.14.a	0.5	29.08	59.6171	4.8751
Fig. 6.14.b	0.1	4.70	12.3733	4.5712
Fig. 6.14.c	0.001	0.16	4.8229	5.1794

Table 6.12: Details of equilibrium (fixed T) MC simulations of the system where external field is above critical external field point for $\Delta x = 0.5$,$k_3 = 0$, $\lambda = 1$, h=1.

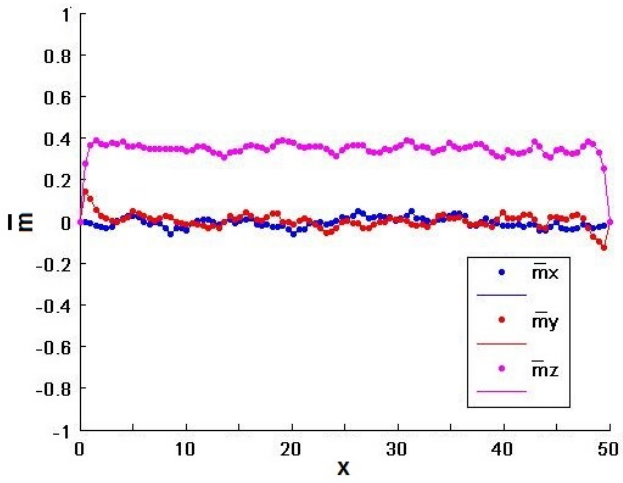

(a)

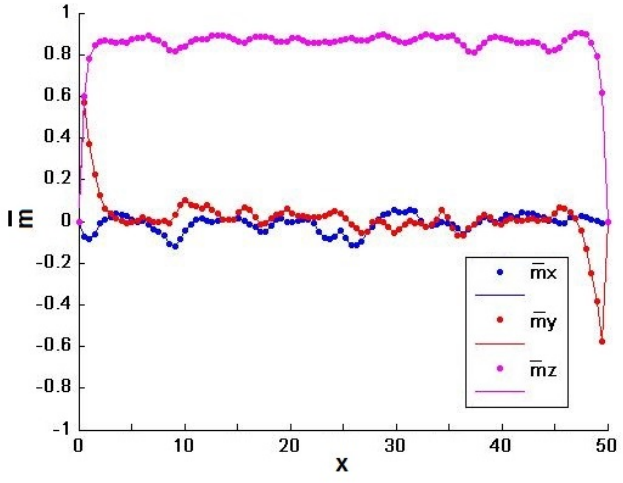

(b)

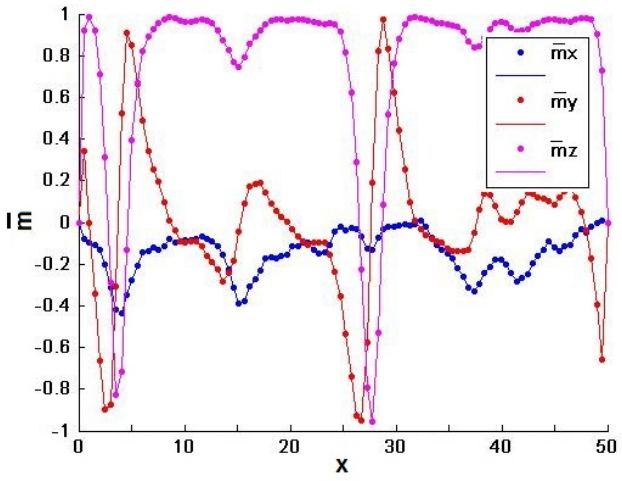

(c)

Figure 6.12: Average spin configuration for the system where external field is above critical external field point (a)T=0.5,(b)T=0.1,(c)T=0.01, for $\Delta x = 0.5$,$k_3 = 0$, $\lambda = 1$, h=1.

Conclusions

We have given a theoretical and computational study of the modification of micromagnetic configurations in magnetic materials, due to the presence of Dzyaloshinskii-Moriya interaction (DMI)and the easy-axis anisotropy that appears at the interface of an ultrathin film.

We examined three different systems, A)Domain Wall, B)Dzyaloshinskii-Moriya interaction and Anisotropy and C)Spiral in the presence of External field. In each case both Non-equilibrium and equilibrium states were examined.

After the simulations we came to the conclusion that in the case of a domain wall solution(A) it is interesting to note that DMI does not change the shape of the 1D domain wall but introduces chirality, of a sign fixed by that of λ. For the most favorable chirality, it lowers the energy.

For the system (B) that consists of DMI and easy-axis anisotropy we should note that the value of anisotropy can affect dramatically the behavior of the system. Particularly in the absence of anistropy as well as for an anisotropy value below the critical anisotropy point we have a proliferation of domain walls and the solution is called spiral. Particularly, when a domain wall is inserted in the system ,the energy is reduced below the energy of the ferromagnetic state.

For a system with an anisotropy constant larger than the critical anisotropy point it is clear that the configuration of the system is a domain wall that moves from x>0 to x<0 or vice versa. Each solution for every sign combination of the spins in y,z-direction are equivalent and the choice is random.

Some significant difference between the case of $k_3 = 0$ and $k_3 < k_c$ is that for the second case the presence of DMI term leads the system to spiral solution at T=0 at higher temperatures. Moreover, the energy in this case is much more closer to the theoretical approach. Lastly, in equilibrium we see that the error of the simulation σ is slightly lower in the second case.

Another interesting result concerns the period of a spiral solution. We came to the conclusion that as the value of anisotropy decreases , the period of the spiral decreased too.

Finally, the system (C) where we face total absence of anisotropy and presence of DMI and external field for values of external field below the external field critical point preforms a spiral configuration which favors the $m_z = 1$ direction. For a value above the critical point of external field the spins in the z-direction move in $m_z = 1$ direction.

In conclusion, the results of the 1D model are essential in order to understand results obtained on skyrmions which are the result of the same problem in the two directions (2D). Our current and future work is to study the nature and the properties of magnetic chiral skyrmions using Monte Carlo simulation methods.

Bibliography

[1] S. Komineas and N. Papanicolaou, "Skyrmion dynamics in chiral ferromagnets," *Physical Review B*, vol. 92, no. 6, p. 064412, 2015.

[2] S. Komineas and N. Papanicolaou, "Topology and dynamics in ferromagnetic media," *Physica D: Nonlinear Phenomena*, vol. 99, no. 1, pp. 81–107, 1996.

[3] S. Blundell, *Magnetism in condensed matter*. Oxford Univ. Press, 2001.

[4] L. Landau, E. Lifshits, and L. Pitaevskiui, *Statistical Physics*. No. Part 2 in Course of theoretical physics, Pergamon, 3rd edition, 1980.

[5] A. Thiaville, S. Rohart, É. Jué, V. Cros, and A. Fert, "Dynamics of dzyaloshinskii domain walls in ultrathin magnetic films," *EPL (Europhysics Letters)*, vol. 100, no. 5, p. 57002, 2012.

[6] M. Lucassen, "Rigid domain wall motion," *Utrecht University*, 2008.

[7] W. K. Hastings, "Monte carlo sampling methods using markov chains and their applications," *Biometrika*, vol. 57, no. 1, pp. 97–109, 1970.

[8] C. Robert and G. Casella, *Monte Carlo statistical methods*. Springer Science & Business Media, 2013.

[9] H. E. Stanley, "Dependence of critical properties on dimensionality of spins," *Physical Review Letters*, vol. 20, no. 12, p. 589, 1968.

[10] X. Yu, Y. Onose, N. Kanazawa, J. Park, J. Han, Y. Matsui, N. Nagaosa, and Y. Tokura, "Real-space observation of a two-dimensional skyrmion crystal," *Nature*, vol. 465, no. 7300, pp. 901–904, 2010.

[11] S. Rohart and A. Thiaville, "Skyrmion confinement in ultrathin film nanostructures in the presence of dzyaloshinskii-moriya interaction," *Physical Review B*, vol. 88, no. 18, p. 184422, 2013.